ACTA ACUSTICA UNITED WITH ACUSTICA
Vol. 90 (2004) 945 – 965

Plucked Guitar Transients: Comparison of Measurements and Synthesis

J. Woodhouse
Cambridge University Engineering Department, Trumpington St, Cambridge CB2 1PZ, UK.
jw12@eng.cam.ac.uk

Summary
The predictions of a calibrated synthesis model for the coupled string/body vibration of a guitar are compared with measurements. A reasonably good match is demonstrated at low frequencies, except that some individual decay rates of "string modes" are hard to match correctly. It is shown to be essential to use an accurate damping model for the string: the intrinsic damping of the classical guitar strings used here is found to vary by an order of magnitude in the audible frequency range. At higher frequencies, two phenomena not included in the synthesis model are found to produce disparities between measurement and synthesis. First, the two polarisations of string motion show modal frequencies which are split further apart than can be explained by body coupling. This effect is tentatively attributed to slight rolling on the fret and/or bridge, resulting in different effective lengths for the two polarisations. Second, unexpected extra peaks are seen in the measured spectra, which are frequency-doubled relatives of the expected peaks due to transverse string resonances. The non-linear mechanism creating these additional peaks is presumed to involve excitation of longitudinal string motion by the transverse vibration.

PACS no. 43.40.Cw, 43.75.Gh

1. Introduction

When a note is plucked on a guitar string, the resulting sound consists of a free transient decay representing the coupled string/body vibration of the instrument. Any attempt to understand guitar sound must rest on an ability to predict the amplitudes, frequencies and decay rates making up this transient signal, given information about the string, the instrument body and player's pluck gesture. This is true whether the aim of understanding is to assess which structural features of the guitar body contribute to audible differences of sound, or to explore the range of different sounds available to the player, or to perform high-quality synthesis of guitar sounds. It should be emphasised at the outset that, throughout this paper, the word "body" is used to include the effects of the surrounding air, both within the cavity and outside. The coupled air-structure modes will be referred to as "body modes" for brevity.

In a companion paper [1], methods were investigated for synthesis of the linear response of a coupled string and body to a pluck. It was demonstrated that reliable and reasonably fast synthesis can be carried out which covers the frequency range of relevance to notes on a classical guitar, up to at least 5 kHz. The general features one would expect to see in a pluck, based on this theoretical modelling, can easily be summarised. The string on its own, with rigidly fixed ends, would have a series of resonances with approximately harmonic spacing and relatively low damping. The frequencies will not be exactly harmonic because of the effect of bending stiffness. Each string "harmonic" is in fact a pair of modes, because the string can vibrate in two different polarisation planes. When the string is coupled to the guitar body through the bridge (and to a lesser extent through the fingerboard), this set of string modes will couple to the set of modes of the unstrung body.

Provided the coupling is not too strong, one would expect most of these coupled modes to be identifiable as either predominantly "string modes" or predominantly "body modes", in the sense that most of the kinetic energy will be concentrated in the string or the body (including the surrounding air) respectively. "String modes" will be expected to have lower damping than "body modes", and to remain approximately harmonically spaced – if they did not, the resulting sound would not be perceived as having a strongly tonal quality. Each "string mode" will still appear as a doublet, with two orthogonal planes of polarisation, but now the two frequencies are likely to be slightly different because the coupling to the body breaks the rotational symmetry of the string. Similarly, the two modes are likely to have different damping factors. This might produce a decay profile of the sound of that "harmonic" showing a double-exponential shape: the early part of the decay could be dominated by the louder but faster-decaying component, but in time the slower-decaying component would take over. If so, this could be significant for the sound of the instrument, since similar decay profiles in the sound

Received 1 October 2003,
accepted 26 March 2004.

of the piano and harpsichord (arising mainly from the use of multiple strings for a single note [2]) are known to be perceptually very important.

In the next section, a first examination of data from guitar plucks will reveal that these expectations are oversimple. The experimental methods will be described, and the qualitative behaviour illustrated. This will lead to a number of questions, which are then explored by comparison with synthesis. First, in section 3, the synthesis model must be calibrated. This involves another series of measurements, and some interpretation. Then, in section 4, the predictions of synthesis will be compared with the corresponding measurements. Some of the features revealed will turn out to be just as one would expect from the theoretical modelling outlined in the previous paper, but others will be surprising and will require significant extensions of the theoretical modelling. One consequence of this study is that a range of psychoacoustical issues arise, associated with which of the features have audible consequences. Such questions are not addressed in this paper, but are good candidates for further study.

2. Measured pluck responses

Measurements of pluck response are simple to make. A string can be played in the usual way with a fingernail, or for a more controlled "pluck" the string can be pulled aside with a loop of fine copper wire which snaps very abruptly at a repeatable level of stress, imparting a step function of force to the string in a precisely known direction. The vibration response can be recorded via the radiated sound, using a microphone, or by using an accelerometer or other sensor on the structure. Measurements of two types will be used in this study. To assess the accuracy of the synthesis models, wire-break plucks and structural measurements give the most precise test. On the other hand, it is very appealing to enquire how much can be learnt about a particular guitar using only microphone measurements and "normal" playing, and data of this kind will also be examined.

Provided that the vibration is linear, the set of frequencies and decay rates arising from a particular string stopped at a particular fret should be the same whatever combination of excitation and measurement is used. As explained above, the apparent decay rate of a given "string overtone" may depend on what mixture of the two polarisations is excited, but if the two relevant "string modes" can be separated in the observation they will always show the same frequencies and decay rates. The pattern of modal amplitudes will, however, vary depending upon the plucking point and details of the pluck gesture. Also, the structural response will differ from the radiated sound because of the differing radiation efficiencies of the body modes.

Once a pluck response has been captured, it can be analysed in several different ways to extract information of different types. Most directly, the time history can be examined with no further processing. Comparisons with synthesis can be made this way, and also evidence of some kinds of transient events may be seen most clearly in the time domain. For example, even for a pluck which sounds satisfactory it can happen that the string makes contact with a fret during the vibration. Such a contact is plainly visible in the signal from a small accelerometer on the guitar bridge, as a burst of very high-frequency signal. Such a burst indicates that the particular pluck should not be used for detailed comparisons with synthesis, because it contains an element not included in the theoretical model.

The next level of processing is to obtain a fine-grained frequency spectrum of the signal using an FFT of sufficient length that the motion has decayed to low amplitudes within the segment analysed, to avoid leakage errors. A time of 5–10 seconds is needed for a typical note on a classical guitar. The spectrum can reveal the pattern of peak heights and frequencies, but it is less well suited to accurate determination of decay rates: the peaks of "string" resonances are so narrow that accurate measurements of bandwidth are not easy. An alternative style of processing, better suited to this task, is to use time-frequency analysis. A sonogram of the pluck signal can be analysed to extract accurate frequencies and decay rates of the various "string" overtones. The approach can reveal aspects of the behaviour which are not clear in the ordinary frequency spectrum. Indeed, it can be helpful to look at more than one type of sonogram: by varying the length of the individual time segments analysed, the trade-off between time resolution and frequency resolution can be controlled [3]. (The sonogram is by no means the only signal-processing option for this task, but it was selected here because of the availability of pre-existing software.)

The first stage of this investigation is to examine some results from "typical" plucks, to illustrate the range of phenomena and to highlight a number of questions which will be addressed by comparison with synthesis. The test guitar is a flamenco instrument with a scale length of 650 mm, and for the purpose of measurements it was held in foam-padded supports at the waist and the head. Controlled pluck responses were recorded using the wire-break method at a distance of 20 mm from the bridge. Each of the six strings was plucked six times: three times for the open string and three with the string stopped at the second fret using a capodastro (cejilla). Each set of plucks used three different angles to the plane of the soundboard: 0°, 45° and 90°. (All plucks were perpendicular to the *string*, of course.) During each measurement the other five strings were thoroughly damped using a thin fibrous sheet woven between the strings but not touching the fingerboard. The resulting vibration was measured with a small accelerometer (Bruel and Kjaer type 8307, weight 0.7 g) fixed to the tie-block of the bridge as close as possible to the point where the relevant string crosses the bridge saddle. This acceleration signal was captured by a data-logger at a sampling rate of 40 kHz.

The resulting data set is quite voluminous, and it is not easy to convey the full range of information which it contains. Two particular notes have been chosen for illustration: B_2 (123.5 Hz) on the second fret of the fifth string,

Table I. String properties for D'Addario Pro Arté "Composites, hard tension" guitar strings, with a scale length of 0.65 m.

String:		1	2	3	4	5	6
Tuning note		E_4	B_3	G_3	D_3	A_2	E_2
Frequency	f_0 (Hz)	329.6	246.9	196.0	146.8	110.0	82.4
Tension	T (N)	70.3	53.4	58.3	71.2	73.9	71.6
Mass/unit length	ρ (g/m)	0.38	0.52	0.90	1.95	3.61	6.24
Wave speed	c (m/s)	429	321	255	191	143	107
Wave impedance	Z_0 (Ns/m)	0.164	0.166	0.229	0.373	0.517	0.668
Bending stiffness	B (10^{-6} Nm^2)	130	160	310	51	40	57
Loss coefficients	η_F ($\times 10^{-5}$)	40	40	14	5	7	2
	η_B ($\times 10^{-2}$)	2.4	2.0	2.0	2.0	2.5	2.0
	η_A (s^{-1})	1.5	1.2	1.7	1.2	0.9	1.2

Corrected Table (figures in original paper were printed incorrectly).

and B_3 (247.0 Hz) on the open second string. (The standard tuned notes of all strings for a classical/flamenco guitar are listed in Table I.) One reason behind this choice of plucks to illustrate is that the second string is representative of the three upper strings, made of monofilament nylon, while the fifth string is representative of the lower strings, constructed with a stranded nylon core overwound with metal wire. The particular strings used in this test were D'Addario Pro Arte Composites, "hard tension". The strings were new when the test was made – with age, the damping of the wound strings tends to increase as a result of damage and contamination penetrating the windings [4]. The strings had been fitted for a few days, enough time for the nylon to stop creeping [5], but they had been played only enough for tuning purposes: the strings were tuned using a standard electronic tuner immediately prior to each measurement, to normal playing precision.

Figure 1 shows the first 17 ms of the two chosen notes, when plucked at an angle of 45°. When the string is plucked, a pair of "kinks" are generated which travel out from the plucking point in opposite directions, and then reflect back and forth along the string. The sharp downward pulses visible in Figure 1 show the times when these kinks reflect from the bridge. The dispersion produced by bending stiffness of the string modifies the shape of the pulses, since the higher frequency components travel faster, leading to a chirp-like "precursor" before each pulse [6]. A clearer view of these precursors will be given later, in Figure 17. The rest of the waveforms, between the pulses, show the effect of body vibration excited by the string vibration. It is apparent to the naked eye that the first period or two in each case contains some high frequency signal, showing as "fuzz" in the plot, which dies away very rapidly.

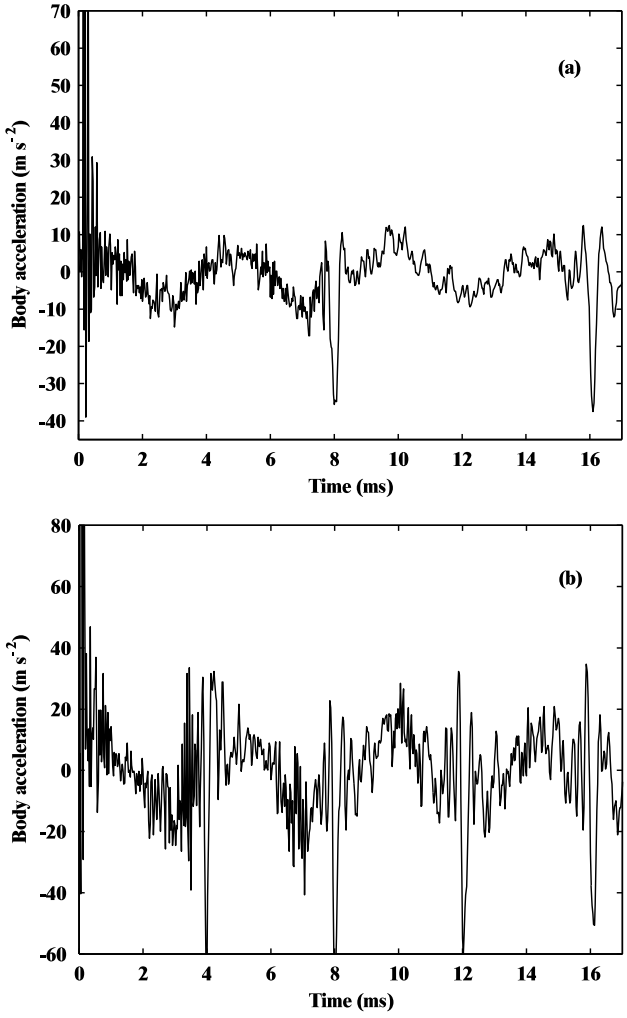

Figure 1. Representative waveforms of guitar plucks from (a) B_2 on the second fret of the 5th string; (b) B_3 on the open 2nd string. The strings were plucked by a breaking wire, at a distance of 20 mm from the bridge and an angle of 45° to the soundboard. Body response was measured by small accelerometer on the bridge near the string attachment point. Acceleration amplitude is normalised to a pluck amplitude of 1 N.

Figure 2 shows the frequency spectra of the two plucks over a wide frequency range up to 18 kHz. Figure 2a, for the note on the 5th string, shows recognisable peaks up to approximately 6 kHz, at which point they disappear below the background noise level until a few peaks rise above it again around 10 kHz. Figure 2b, for the note on the 2nd string, shows clear peaks extending up to 16 kHz. This is perhaps a surprise: the immediate impression on listening to these notes is that the (new) overwound string produces a timbre with more "twang", whereas the monofilament string is a little more "mellow". This figure indicates

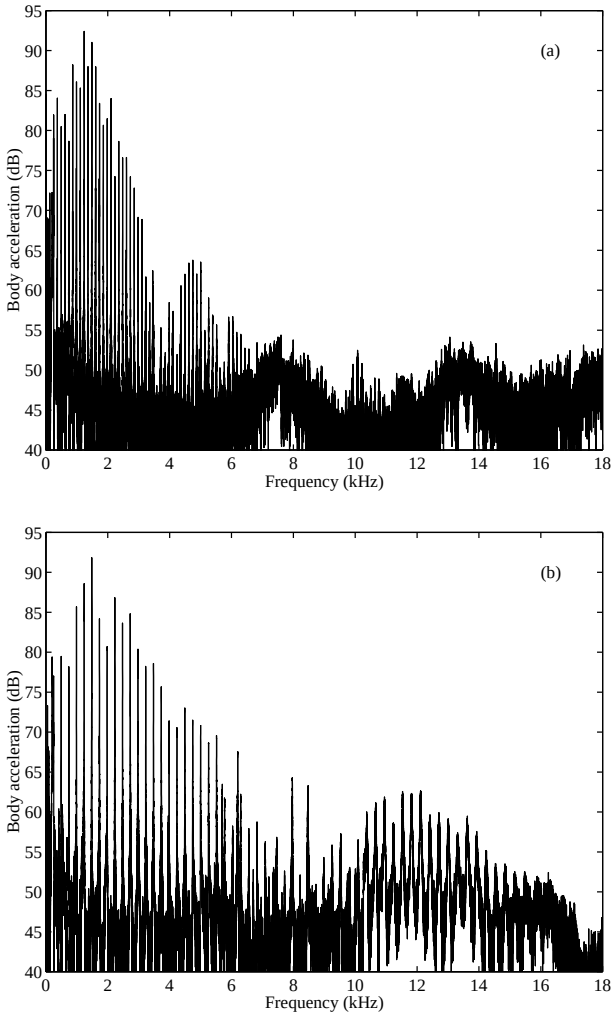

Figure 2. Frequency spectra of the two plucks shown in Figure 1: (a) B_2 on the second fret of the 5th string; (b) B_3 on the open 2nd string. Plots show the amplitude spectra of the normalised data from Figure 1 following an FFT of length 131072 samples.

that "twang" is not directly associated with increased high-frequency content, rather to the contrary.

Looking closely at Figure 2b, one gets a first indication of a phenomenon which was consistently seen in all the pluck results. At lower frequencies, up to about 5 kHz in this case, a row of peaks can be seen which look roughly equally spaced as one would expect. However, in the range 5.5–10 kHz this gives way to a pattern which, even on this small scale, can be seen to be more irregular. From 10–16 kHz the regular pattern returns. The data of Figure 2a shows a generally similar pattern, but it is barely discernible in a plot of this resolution. The irregular portion of the pattern occurs in the range 3–6 kHz in this case. To see more of what is happening in these spectra requires a more detailed view.

Figure 3 shows selected parts of the spectra of Figure 2, together with corresponding results for the other two plucking angles for each note. The solid lines show the plucks normal to the soundboard, giving curves which are almost invariably the highest in each case. The dashed curves show the 45° plucks, as in Figure 2, and these are generally close to the solid curves but a little lower. Finally, the dash-dot curves show the response to plucks parallel to the soundboard, which usually have significantly lower levels as one would have guessed.

Similar general features are revealed for both notes. The two upper plots, for low frequencies, show sharp "string" peaks as expected; two in Figure 3a and one in Figure 3b. Apart from these, the plots show clear evidence of body vibration. The same set of body mode frequencies appear, with varying amplitudes, in all three plucking directions and for both notes (except where obscured by the noise floor of the measurements, into which the lowest curve in particular dips quite often).

A little higher in frequency, the middle two plots show a narrow frequency range which includes just one nominal "string mode" frequency. The plots show that in both cases the "string" peak is split into a pair, spaced a few Hz apart. The higher-frequency peak of each pair shows strongly in the normal-direction pluck, while the lower frequency shows most clearly in the pluck parallel to the soundboard. The plucks at 45° show signs of both peaks. In this frequency range, no clear effect of body vibration is evident.

At higher frequencies still, the two lower plots show some details of the "non-regular" part of the spectrum mentioned above. These plots show a 200 Hz range, as in the top pair of plots, so that one would expect to find two pairs of "string peaks" in Figure 3e, and one pair in Figure 3f. Instead, the pattern of peaks shows unexpected and complex structure, with clusters of peaks in the general vicinity of the expected string "harmonics" in both cases. There are four clear peaks in Figure 3f, and perhaps two groups of four in Figure 3e.

Moving on to illustrate another style of analysis, Figure 4 shows a sonogram of the open string pluck, computed using individual FFTs of length 0.1 s. The plot shows amplitude in decibels as a function of frequency and time, from the instant of the initial pluck. The dynamic range of the plot has been limited by a preset "floor" so that the main features are not obscured by noise. Nine "string harmonics" are clearly visible in this range, together with some evidence of transient body vibration at early times, particularly at low frequencies. It is straightforward to identify the "string modes" and extract the decay profile of each by taking an appropriate section through the sonogram. The results for the first nine modes are shown in Figure 5: these simply show level versus time in individual frequency bins corresponding to the obvious "ridges" in Figure 4.

Most of these curves show an underlying trend of exponential decay, many of them with superimposed "beating" behaviour of greater or lesser vigour. The rates of decay vary significantly: linear regression fits are also plotted, from which best-fitted decay rates can be deduced. The "beating" behaviour is the sonogram manifestation of the split peaks seen in Figure 3: the frequency resolution of the sonogram is insufficient to separate closely-spaced pairs of peaks, so they appear in the same frequency bin and beat.

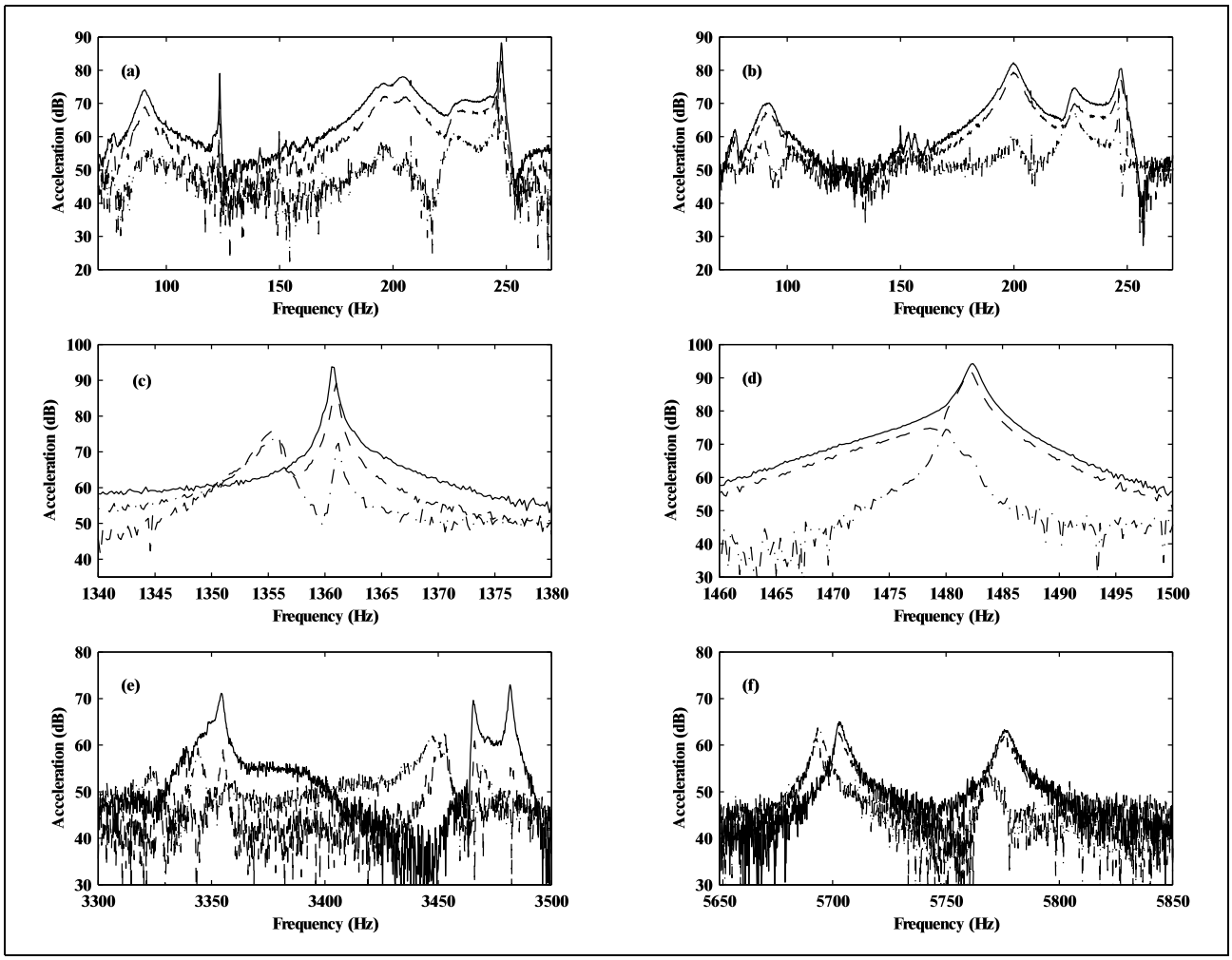

Figure 3. Details of frequency spectra of plucks: (a,c,e) for B_2 on the second fret of the 5th string; (b,d,f) for B_3 on the open 2nd string. In each case the solid line (usually the upper trace) shows a pluck normal to the soundboard, the dashed line (usually the middle trace) shows a pluck at 45°, and the dash-dot line (usually the bottom trace) shows a pluck parallel to the soundboard.

In particular, the sixth plot in Figure 5 corresponds to the split peak seen in Figure 3d. What is *not* seen in Figure 5 is any convincing example of "double exponential decay", which, as was explained in section 1, might arise from different decay rates of the two polarisations of string motion. The decay profile for the lowest frequency has something like the "double decay" shape, but in this case the almost horizontal trend at later times is probably an artefact of the measurement noise floor rather than a true decay rate of string motion.

The next stage of the analysis of decay rates is to gather together the results for all available "string modes" and look for interesting behaviour of a global nature. A note can be played on a given string stopped at each fret in turn, and each analysed in the manner of Figures 4 and 5. The decay rates can be collected, sorted into frequency order, and plotted to give the results shown in Figure 6. Every note up to the 12th fret on each string of the test guitar has been played, and analysed. A separate curve is plotted in the figure for each string, to show decay rate as a function of frequency. Decay rates, if governed by linear theory, do not depend on the details of the pluck or the sensor used, so this measurement can be performed in whatever way is most convenient: in this case using normal playing

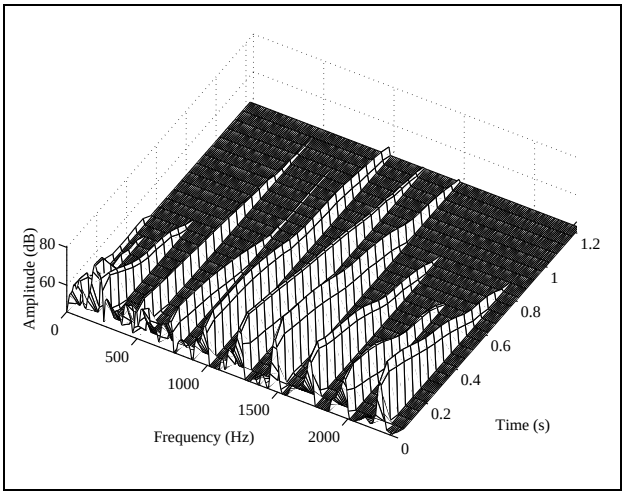

Figure 4. Sonogram of the pluck shown in Figures 1b, 2b, using short-time FFTs of length 0.1024 s.

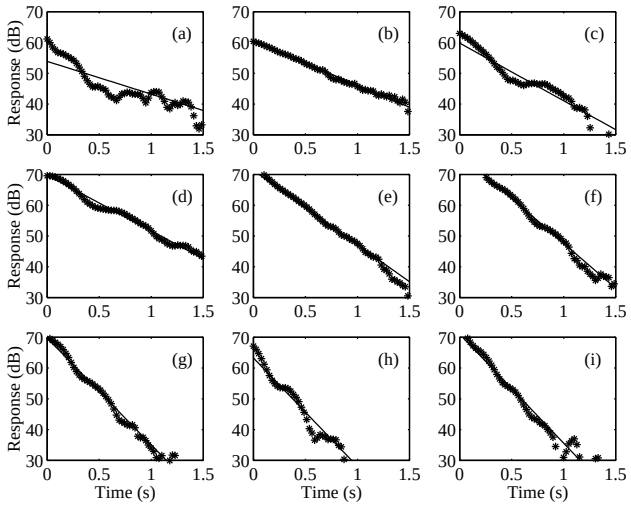

Figure 5. Decay profiles of the nine main ridges from Figure 4, corresponding to the first nine "string" overtones at frequencies of 247.2 Hz, 493.9 Hz, 741.1 Hz, 988.4 Hz, 1236 Hz, 1484 Hz, 1732 Hz, 1980 Hz and 2229 Hz. Best-fitted exponential decays are shown as straight lines: these correspond to Q-factors 631, 939, 1073, 1487, 1396, 1382, 1361, 1531 and 1730 respectively.

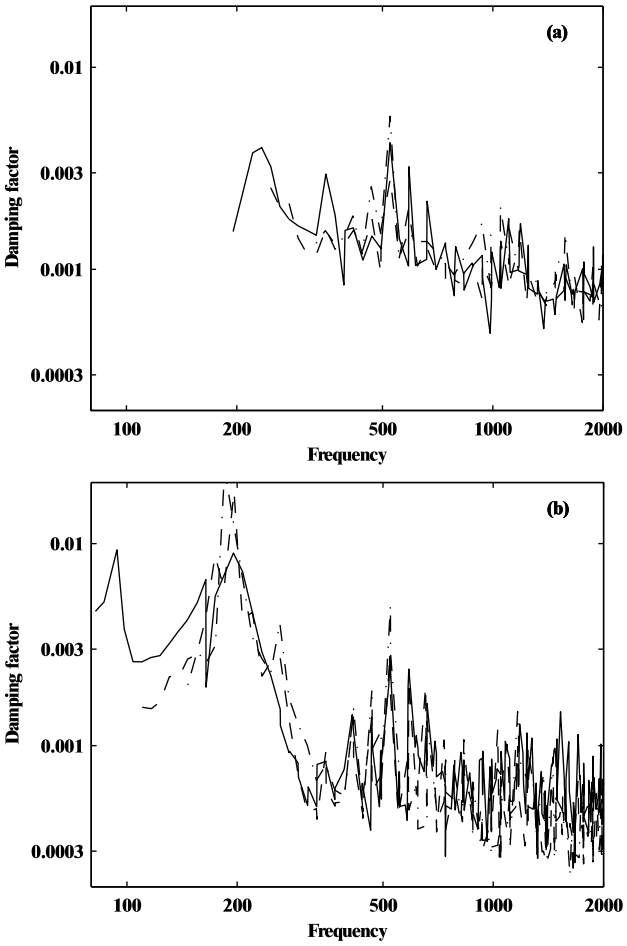

Figure 6. Damping factor as a function of frequency, measured from "string modes" of all notes up to the 12th fret on the test guitar. (a) The three upper strings: dash-dot line: first string; dashed line: second string; solid line: third string. (b) The three lower strings: dash-dot line: fourth string; dashed line: fifth string; solid line: sixth string. These results were measured from normally played notes, by microphone signal in a domestic room.

and a microphone to record the response. It thus represents the closest one can easily come to a useful quantitative measurement based on normal playing, including holding the guitar in the conventional manner rather than using an artificial support rig of some kind.

What is actually plotted in Figure 6 is the loss factor, the inverse of the Q-factor. The "floor" envelope of this figure presumably shows the intrinsic loss factor of the string, while the peaks rising above this floor show increased damping as a result of energy loss to the guitar body. Large peaks would be expected to correspond to body resonances with significant amplitudes at the bridge. Of course, these peaks are not resolved very clearly because the frequency values available are only those produced by the strings when playing notes of the equal-tempered scale at the usual pitch standard of A 440 Hz. To achieve more smooth curves, the test would have to be repeated with the strings progressively detuned, but this has not been attempted. However, in the companion paper [1], a similar string-tuning exercise was carried out using synthesis rather than measurements, and the result can be seen in Figure 7 of that paper. A factor complicating the interpretation of Figure 6 is that it may not be clear which of the two string polarisations determines the result, and it is possible that different plucks of the same note might yield a different loss factor for a given "string overtone" if the dominant polarisation changed.

One fact immediately evident is that the three top strings, shown in Figure 6a, show very similar loss factors, while the three lower strings shown in Figure 6b show values similar to each other, but significantly different from the top strings. This pattern of damping factors is probably a key factor in producing the very marked change in tonal quality between the 3rd and 4th strings. However, it is not the only factor: it will be seen in section 3.3 that the bending stiffness is also very different between the 3rd and 4th strings.

The general behaviour shown in Figures 1–6 is typical of what has been seen in data gathered from some 10 different guitars. A number of issues are raised by these results. What causes the "cutoff" at about 7 kHz in Figure 2a? What accounts for the peak splitting seen in Figure 3c,d, and in a different guise in Figure 5? What causes the complex pattern of peaks seen in Figure 3e,f? Why are "double exponential decays" not seen (or, more correctly, rarely seen)? Why is the influence of body vibration much more evident at low frequencies than higher ones? Are pluck responses within the range of normal guitar playing well described by linear vibration theory, or are significant nonlinear effects present? Is the pattern of frequencies and decay rates compatible with a theoretical model of the kind normally used, dealt with in some detail in the companion paper [1]? To address all these questions, it is necessary

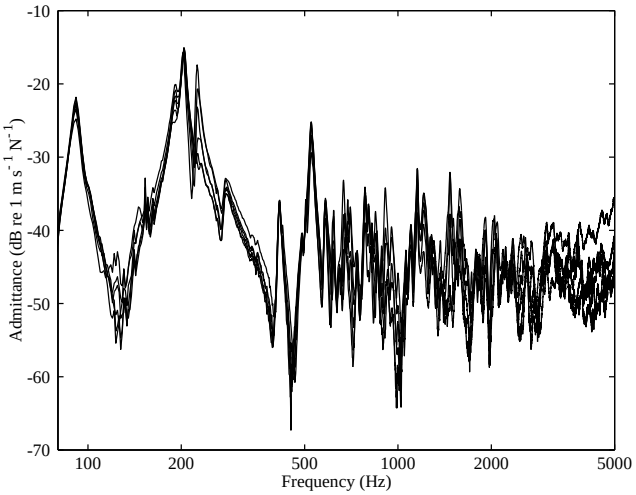

Figure 7. Input admittance at the bridge saddle, measured at the position of each of the six strings.

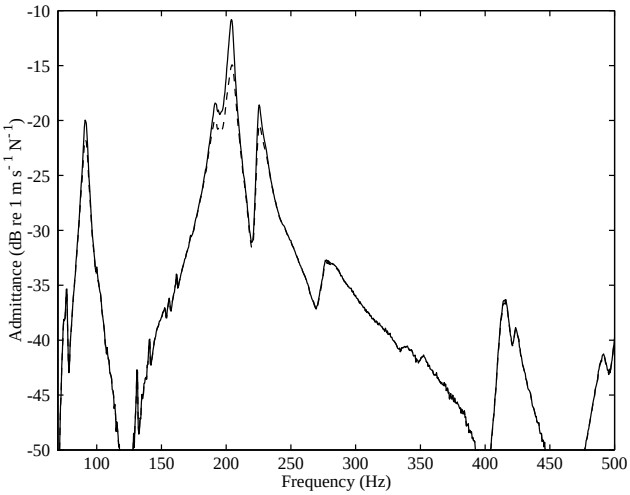

Figure 8. Input admittance at the position of the sixth string (E_1) on the bridge saddle, measured with damped strings (dashed line) and after compensating for the energy loss into the strings (solid line).

to compute synthesised results and compare them with the measured results.

3. Calibration of the synthesis model

As a first stage, the synthesis model must be calibrated to match the string and body behaviour of the test guitar. The information needed is as follows: for the strings, the tension, mass per unit length, bending stiffness and internal damping; and for the body, the 2×2 admittance matrix at the string's contact point on the bridge saddle. The admittance matrix may be used directly or fitted using a modal expansion, depending on the synthesis method to be used. Some of these quantities are straightforward to find, others require care and iteration in the light of all available experimental results.

3.1. Admittance

Determining the body admittance is in principle a straightforward vibration measurement. The input admittance in the direction normal to the guitar's soundboard is indeed easy to measure, for example using a small impulse hammer and a laser vibrometer to sense the response. This method has the advantage that neither the actuator nor the sensor adds any mass, stiffness or damping to the guitar. It is hard to measure exactly at the excitation point by this method because the hammer obstructs the laser beam, but with a miniature hammer (PCB type 086D80) it is possible to drive and monitor at points on the bridge saddle only some 4 mm apart. Measurements of this kind close to the contact points of each of the six strings are shown in Figure 7. The guitar was held in the same support rig described in the previous section for the wire-break pluck tests. As one would expect, the results show similar trends but differences of detail because of the variation of mode shapes along the line of the bridge saddle. The measurements were calibrated in the usual way, by using the same hammer and laser to measure the admittance of a known mass supported by soft foam [7].

One important question about such measurements relates to what should be done with the strings: should they be damped, left undamped, or removed entirely? None of these options is entirely satisfactory. If the strings are undamped, then the measurement is of the coupled string/body behaviour rather than of the body alone, which defeats the object of calibrating a "body model" to use in simulations of the coupled system. If the strings are removed, the bridge saddle is not held properly in place, and if the saddle is removed then the bridge mass is changed. Also, as originally pointed out by Schelleng [8] in the context of violin measurements, the axial stiffness of the strings may contribute to the body vibration characteristics quite separately from the role of the transverse string vibration which is our primary interest.

This leaves only the option which was in fact used in the measurements just shown: to have the strings in place but damped. They will then add some damping to the body modes and potentially give misleading answers. The "worst case" is easily assessed. If the strings were perfectly damped, so that waves travelled out along the string but no reflection ever returned, they would be felt by the bridge as pure resistances, with a value equal to the characteristic impedance of the string. For the strings used in these tests, the impedances are given in Table I. For the purposes of a simple estimate, suppose that all six strings were attached at the same point on the bridge, say at the position of the 6th string. The net effect could then be compensated by taking the body impedance (the inverse of the relevant admittance from Figure 7), subtracting the total string impedance (2.12 Ns/m for the strings used here), and inverting the result to give the body admittance "without the strings". The result of this calculation is shown in Figure 8. The original curve, with damped strings, is shown dashed, while the "compensated" result is shown

solid. The two curves are almost indistinguishable except near the large peaks below 250 Hz. The compensation process reduces the damping of these peaks by a significant amount: for the peak at 91 Hz the Q factor rises from 20 to 25, at 205 Hz it rises from 33 to 47, and at 225 Hz it rises from 49 to 59.

The actual influence of the strings will probably be rather less than this "worst case" calculation. It may be concluded that admittances measured with damped strings can be used with reasonable confidence for synthesis purposes, except perhaps near a few low modes of the body. In practice, there are other factors influencing the damping of these low body modes. It has been observed in the measurements reported here that the low-frequency resonances, and especially their damping factors, are significantly affected by the arrangement used to hold the guitar. This is likely to apply equally strongly to the various ways in which a guitar is held for playing: guitarists use a variety of positions, involving varying degrees of body contact and therefore presumably varying levels of added damping. This question might be worthy of further attention, but for the present purpose it will be ignored and the admittance measurements with damped strings used throughout this study.

An interesting aside concerning input admittance measurements is to compare results for guitars with those for violins. Figure 9a shows the input admittance for three different classical and flamenco guitars at the position of the lowest string. The values are normalised with respect to the characteristic admittance of the lowest string, so the result can be regarded as the string-to-body impedance ratio. The frequency scale is expressed in semitones above the lowest note of the instrument when conventionally tuned. Figure 9b shows similar results for five violins, normalised in the corresponding way. A number of observations can be made from these results. First, all the guitars have a strong family resemblance, as do the violins, but the two are very different from each other. The lowest strong resonance in the playing range is an "air resonance" in both cases. For the violins this shows as a rather small peak in the admittance, around the 7th semitone. In the guitars, the corresponding peak is taller, and falls at lower frequencies, around the 2nd or 3rd semitone: coupling between "air" and "body" motion is much stronger in the guitar than in the violin. Both types of instrument have their highest peaks in a similar region, about 15–20 semitones above the lowest note. The guitars show higher values at this highest peak, several decibels above those for the violins. String-to-body coupling at the peak level of the guitars could probably not be tolerated in a violin because it would cause excessive problems with "wolf notes" [8, 9].

At higher frequencies, though, the position reverses. In the region around 35–50 semitones above the lowest note the violins exhibit a broad hump, which was originally called the "bridge hill" by Jansson [10, 11]. The level there is similar to that at the "main body resonance". In the guitars, by contrast, the level in this region is much lower, some 20 dB below the highest peaks. The reason is presumably to be found in the different methods of exciting the strings in guitars and violins. In the violin, energy is fed in continuously by the bow, so that the design of the instrument can afford to maintain a fairly close impedance match to the strings up to high frequencies, in order to radiate significant sound energy in a region at which the human ear is most sensitive. For the guitar, this is not an option. Once the string has been released, no further energy can be supplied by the player. If the high-frequency energy were extracted too quickly from the strings, the decay rates would be very fast and probably the player would complain that the instrument didn't "sing" – in fact, the result would sound like a pizzicato violin.

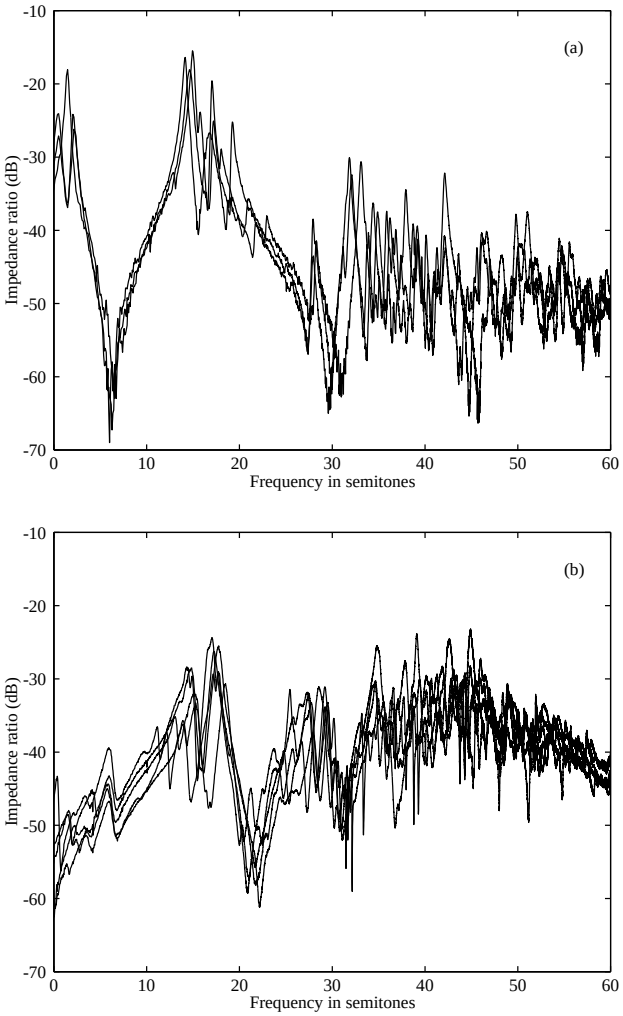

Figure 9. Input admittance for (a) three classical and flamenco guitars and (b) five violins, normalised by the impedance of the lowest string and plotted with a frequency scale based on the lowest note of the instrument.

This immediately explains why a violin can be much louder than a guitar, and why a guitarist has a hard job to play with, for example, a string quartet without being drowned. The guitar is designed to conserve the string's energy at high frequencies for tone-quality reasons. This is achieved, perhaps, by the heavy bridge of a classical guitar, which gives a string-to-body impedance ratio which is

relatively small at higher frequencies. The violin bridge, by contrast, has to be very light in order *not* to have this effect on the impedance ratio, except when mass is deliberately added in the form of a mute. The exception in the acoustic guitar world is the type of jazz guitar which has a tailpiece and a rather light "floating" bridge similar to that of an Italian mandolin. Again, this makes musical sense. These guitars are traditionally played in a more percussive way than classical guitars, particularly when used as accompanying instruments: "singing tone" is presumably at less of a premium, compared with loud and crisp sounds with rapid decay.

Returning to the question of measuring the admittance behaviour needed for the synthesis models, the measurements reported so far are sufficient for a model which considers only the motion of the string normal to the soundboard. However, models which consider both polarisations of the string vibration require the 2×2 admittance matrix. It is convenient to denote the direction normal to the soundboard as "1", and the tangential direction "2". The admittance shown in Figures 7, 8 and 9a is then naturally denoted Y_{11}. The two cross admittances Y_{12} and Y_{21} should be equal by a standard reciprocal theorem [12]. It is possible to measure Y_{12} using the hammer/laser method, by keeping the hammer in the same position as used for the previous measurement and obtaining a laser reflection from the side of the string, aligned parallel to the bridge saddle. However, it proved difficult to measure Y_{22} and Y_{21} by this method. Without attaching something solid to the bridge against which the hammer could strike it is hard to apply an impulsive force with sufficiently broad frequency bandwidth in the direction parallel to the bridge saddle, at the correct position for the string contacts. (However, it may be noted that Lambourg and Chaigne report successful measurements by a similar method [13].)

To determine the full matrix for this study, an alternative measurement method was used. The most satisfactory results were obtained by using the small accelerometer as sensor, and applying force to the string at its contact point with the saddle using the wire-break method. This gives admittance directly: the acceleration response to a step function of force is the same as the velocity response to an impulsive force. It is not easy to measure the force from the breaking wire, but this force has been demonstrated to have good repeatability, so the measurement can be calibrated by re-measuring Y_{11} by this approach, and finding the scale factor necessary to match the (calibrated) hammer/laser measurement. The wire-break force can be applied in any chosen direction, including the desired tangential and normal directions. For response in the normal direction the accelerometer was fixed to the tie-block, as for the pluck measurements. For response in the tangential direction, it was possible to fix the accelerometer on its side to the back of the saddle, between the saddle and the tie-block, so that it responded directly to tangential acceleration. By this approach, the full admittance matrix was measured. The measurement does not have as good a signal-to-noise ratio as the hammer/laser measurement, but it works well enough for the purpose required. The measurement of Y_{11} gave reasonable agreement with the previous measurements by the hammer/laser approach, and the results for the full matrix show good qualitative agreement with those of Lambourg and Chaigne [13].

3.2. Modal fits and the "statistical guitar"

It was shown in the companion paper [1] that the most satisfactory and efficient synthesis method was based on adding impedances in the frequency domain, then performing an inverse FFT to obtain the time response. There are two approaches to the body admittance for this purpose: either the measurements can be used directly, or they can be fitted by a modal expansion. The latter method involves more work and some exercise of judgement at the higher frequencies, but it results in a cleaner set of admittance functions because the fits are performed using the reliable data near the peaks, then the modal formula gives the function at intermediate frequencies where the measured data was obscured by noise. Also, since the full matrix has been measured, the fitting process has some redundancy and therefore contains built-in checks on the reliability of the measurements.

The standard formulae for the admittances in terms of modal parameters can be written in the form

$$Y_{11}(\omega) = \sum_k \frac{\mathrm{i}\omega \cos^2\theta_k}{m_k(\omega_k^2 + \mathrm{i}\omega\omega_k\eta_k - \omega^2)}, \tag{1}$$

$$Y_{22}(\omega) = \sum_k \frac{\mathrm{i}\omega \sin^2\theta_k}{m_k(\omega_k^2 + \mathrm{i}\omega\omega_k\eta_k - \omega^2)}, \tag{2}$$

and

$$Y_{12} = Y_{21}(\omega) = \sum_k \frac{\mathrm{i}\omega \cos\theta_k \sin\theta_k}{m_k(\omega_k^2 + \mathrm{i}\omega\omega_k\eta_k - \omega^2)}, \tag{3}$$

where the kth mode has effective mass m_k, natural frequency ω_k and modal damping factor η_k (or corresponding modal Q-factor $Q_k = 1/\eta_k$). Recall that these "body modes" include not only the structural vibration, but also the effects of the surrounding air. The "effective mass" is related directly to the kth mode shape u_k: if the mode shape is normalised in the usual way with respect to the system mass matrix [12], then

$$m_k = 1/u_k^2 \text{ (bridge)}, \tag{4}$$

where (bridge) connotes the attachment point of the string. Finally, the mode involves motion at the string's attachment point at a particular angle to the normal to the soundboard (i.e. the 1-axis), denoted θ_k. During the process of fitting the measured admittance matrix using modal parameters, each natural frequency and damping factor is determined by the position and shape of the resonant peak (for example using circle fitting [7]). Then from the amplitudes of the peak in the three measured admittances the two parameters m_k and θ_k are determined – this is where the redundancy appears, since two parameters must fit three measurements. For example, the two values can

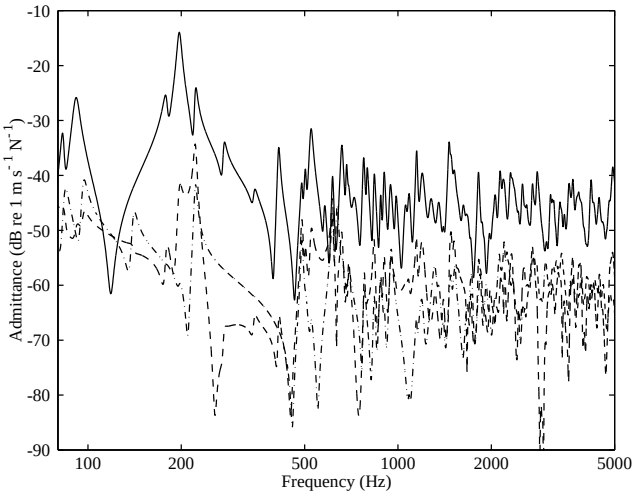

Figure 10. Admittance matrix at the position of the sixth string (E_1) on the guitar bridge, based on modal fitting to measurements up to 1.4 kHz and using a "statistical fit" (see text) above that. Solid line: Y_{11}; dash-dot line: Y_{22}; dashed line: Y_{12}.

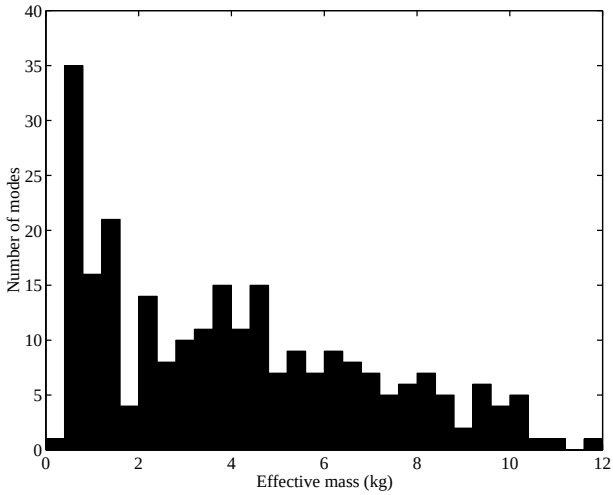

Figure 11. Histogram of effective modal masses used to compute the admittances of Figure 10.

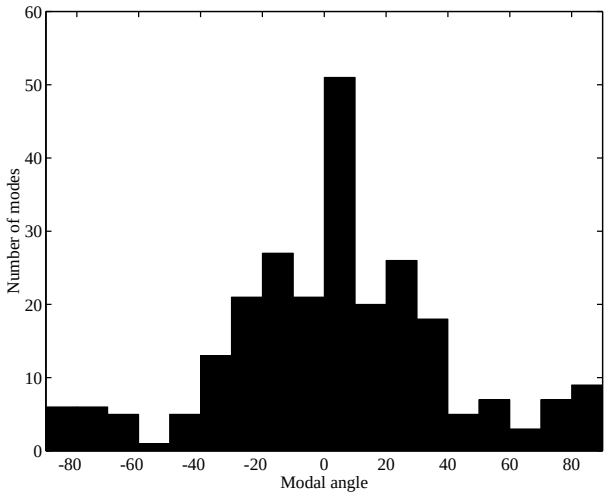

Figure 12. Histogram of modal angles θ_k used to compute the admittances of Figure 10.

be determined using Y_{11} and Y_{22}, then Y_{12} should match automatically, serving as a consistency check.

This fitting process was carried through for the first 51 modes of the system (including some low-frequency modes associated with the support arrangements), giving a satisfactory fit to all three admittance measurements up to about 1400 Hz. By this frequency the modal overlap of the system is significant [14], and it becomes increasingly difficult to recognise and fit individual modes. Instead, a "statistical" approach was taken to extending the model to higher frequencies. Rather than trying to fit the exact behaviour of this particular guitar, admittance functions were calculated using a random number generator in such a way as to create an admittance matrix which shares a range of statistical properties with the actual guitar. It probably has as much in common with the real guitar as would two guitars made by the same luthier with the aim of making identical instruments. It will be seen that this is an adequate level of description to resolve some of the key questions raised at the end of section 2.

In the "statistical range", all the modal properties are generated by random processes. The natural frequencies are chosen by a random process which gives the correct average modal density and the expected Rayleigh distribution of spacings between adjacent frequencies [15]. The average frequency spacing for the modes fitted explicitly was found to be 38 Hz. For a plate-like structure (ignoring the influence of modes of the internal air cavity [16]) the modal density is expected to be constant so this mean spacing is used for the higher modes. Each increment of frequency was thus calculated using the expression

$$\Delta f = 38 \cdot (2/\pi)\sqrt{r_1^2 + r_2^2}, \qquad (5)$$

where r_1 and r_2 are two numbers randomly drawn from a Gaussian population with zero mean and unit standard deviation. The other modal properties were calculated by simpler methods. The Q-factors are selected from a uniform distribution between 30 and 80, and the modal amplitudes from uniform distributions matched to the ranges found for the modes fitted deterministically. The resulting admittances are plotted in Figure 10. Histograms of the distribution of modal masses m_k and modal angles θ_k for the fitted model are shown in Figures 11 and 12 respectively.

A final remark on the modal fitting concerns the possibility of complex mode shapes. The theoretical models developed in the companion paper [1] made an assumption of "proportional damping" so that the mode shapes, and hence the effective masses from equation (4), are real. However, the guitar body stucture will undoubtedly have different internal damping in the different woods used for different parts. Also, the "body modes" include the effect of the inside the cavity and surrounding the body, and this will have different damping properties again. These effects will lead to non-proportional damping and thus to complex

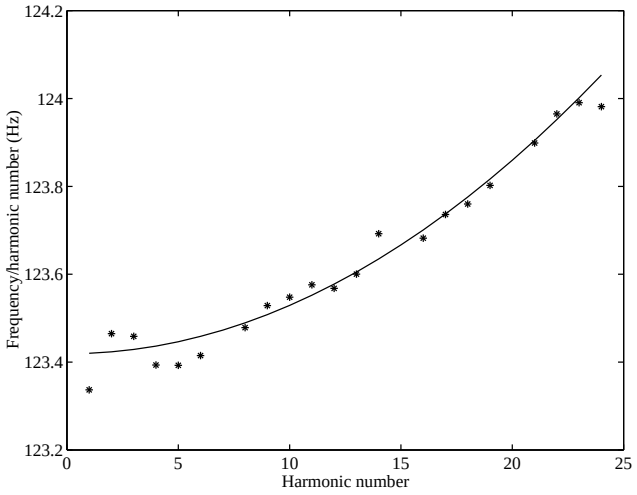

Figure 13. Frequencies of "string modes" divided by "harmonic number" n for a pluck normal to the soundboard of the note on the second fret of the fifth string (solid symbols), together with the best-fitted curve corresponding to equation (6).

mode shapes [7]. However, in practice the modal fitting process just described was carried through using real mode shapes and real effective masses, and a satisfactory fit was obtained to the measured admittances. The modes show a small degree of complexity, as is usually found in any experimental modal test, but the effects on the admittance are small and can be neglected for the present purpose.

3.3. Fitting the string parameters

The manufacturer's web site provides values for tension and mass per unit length of the strings. The wave speed and the characteristic impedance can be deduced from these. These values are all given in Table I for the strings used here. The bending stiffness must be measured, but it can be easily determined from measurements of overtone frequencies, fitted to the well-known theoretical result for a stiff string [17]. A typical example is shown in Figure 13. The note chosen is B_2 on the second fret of the 5th string, plucked normal to the soundboard. The first 24 "string modes" have been analysed by the sonogram method. The modal frequencies are required to a higher accuracy than that given by the spacing of the FFT bins from the sonogram, since this is based on short FFT analysis. A more accurate value of each frequency can be found by analysing the variation of phase as a function of time in the relevant frequency bin. If the signal in this bin is dominated by a single decaying sinusoid, the phase should vary linearly in time with a gradient which can be fitted by linear regression. This gradient can be used to correct the rough frequency estimate given by the bin-centre frequency. For each "string mode" giving a satisfactory fit, a point is plotted in Figure 13 to show the ratio of frequency to "harmonic number" as a function of "harmonic number".

In the absence of bending stiffness the points would lie near a horizontal line in this plot, indicating "string" frequencies which were only disturbed away from exact harmonic relations by the influence of coupling to the body vibration. What is in fact seen is a parabolic curve, since the effect of bending stiffness (assumed to be small) leads to progressive sharpening of higher overtones, such that the nth "string frequency" is given by

$$f_n \approx n f_0 \left(1 + \frac{B\pi^2}{2ZL^2} n^2\right), \tag{6}$$

where f_0 is the fundamental frequency, B is the bending stiffness, T is the tension and L is the string length. By best-fitting this quadratic function of n to the data points, as shown by the solid line in Figure 13, a value of the bending stiffness B can be deduced. By repeating the measurement at each fret on a given string an average value can be found, and this gives the best estimate of the stiffness. These average values for each string are listed in Table I. For the three top strings, which are solid cylinders with no layered structure, a value of Young's modulus E can be deduced if desired, since $B = EI$ where the second moment of area I is given in terms of the radius a by

$$I = \pi a^4/4. \tag{7}$$

The values of E determined in this way are comparable with those measured by Chaigne [5]. For the three lower strings the bending stiffness cannot be interpreted in this simple way, since the string construction is more complicated.

In a study by Järveläinen *et al.* [18], musical notes with varying degrees of inharmonicity having the form of equation (6) were synthesised, and a threshold of audibility determined. This threshold takes the form of a critical value of the parameter $B\pi^2/2TL^2$ such that the sound is perceptibly different from that of a perfectly harmonic string. It is interesting to compare this threshold with the values measured for the guitar strings. Figure 14 shows the result, in the form of plots of the factor by which the measured value exceeds the threshold. Because the threshold from [18] was found to be frequency dependent, the value of this factor varies, for a given string, depending on which note is played, so the plots are expressed as a function of fret number. The conclusion is that inharmonicity caused by bending stiffness should be clearly audible for all strings, most strongly for the sixth and third strings. The general trend across the strings is that inharmonicity becomes more audible towards lower notes, but there is a significant jump in the opposite direction between the fourth and third strings. This may be another contributory factor to the clear contrast of sound quality between these strings.

The hardest of the string properties to determine reliably is the internal damping behaviour. Valette [19] has shown measurements which reveal strong frequency dependence of the damping of musical strings, and he has also discussed a variety of physical mechanisms responsible for internal damping. Measurements on the strings of the test guitar reveal frequency variation very similar to that shown by Valette, and a model of the general form he suggested can be fitted to these results.

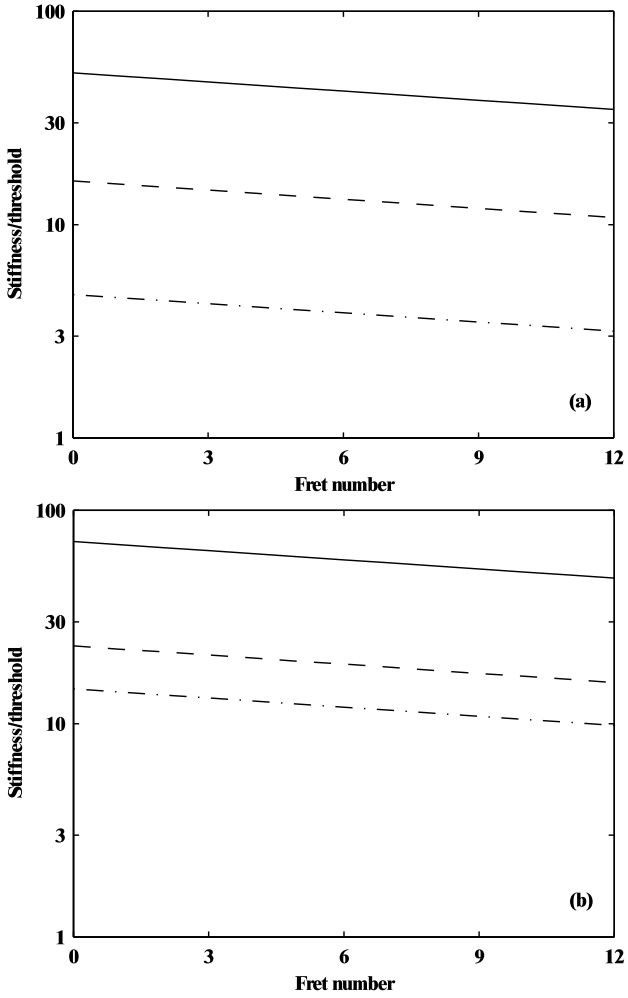

Figure 14. Factor by which the inharmonicity due to bending stiffness of the test guitar strings rises above the threshold value for audibility from reference [18]. (a) The three upper strings: dash-dot line: first string; dashed line: second string; solid line: third string. (b) The three lower strings: dash-dot line: fourth string; dashed line: fifth string; solid line: sixth string.

The model to be used here contains three parameters associated, at least notionally, with three damping mechanisms. These are: viscous damping due to movement of the string through the air, "internal friction" associated either with macroscopic rubbing (in the multi-stranded and overwound strings) or with inter-molecular effects (in the monofilament strings), and energy loss associated with the bending stiffness (i.e. a complex Young's modulus). By lumping the first two terms together and regarding them as a frequency-dependent "complex tension", then using a small-damping argument based on Rayleigh's principle as described in section 3.1 of the companion paper [1], an expression for the loss factor of the nth mode of the string can be obtained in the form

$$\eta_{sn} = \frac{T(\eta_F + \eta_A/\omega_n) + B\eta_B(n\pi/L)^2}{T + B(n\pi/L)^2}, \qquad (8)$$

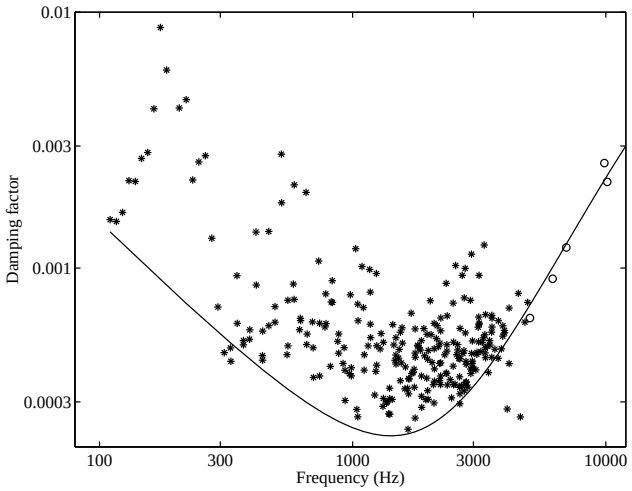

Figure 15. Damping factors measured from "string modes" of notes up to the 12th fret on the sixth string (E_1) of the test guitar (plotted symbols) and the fitted version of equation (8) which follows the "floor" of these data points (continuous curve).

where η_F, η_A and η_B are the coefficients determining "friction", "air" and "bending" damping respectively, and $\omega_n = 2\pi f_n$ is the angular frequency of the mode.

This approach should be understood as a combination of physically-based modelling and curve-fitting, since the physical mechanisms are not understood in sufficient detail to provide a fully convincing predictive model. In particular, the form and origin of the "air damping" term is open to question. However, it will be seen shortly that the damping of the strings definitely rises at lower frequencies, and a term with this simple $1/\omega$ functional form gives an *ad hoc* fit which seems good enough for present purposes. Similarly, both the "internal friction" and "bending" terms are likely in reality to vary with frequency, and the assumption of constant coefficients here is purely a matter of pragmatic convenience. Many issues are raised which would merit further study, since the damping of musical strings almost certainly has a strong influence on their sound. For example, how accurate is equation (8), and how do the coefficients η_F, η_A and η_B vary with string materials and construction, or with age and wear? Only very limited information on such questions is available in the current literature (see for example [4, 19]).

The fitting process for this damping model is illustrated in Figure 15, for the 5th string of the test guitar. The stars mark the frequencies and damping factors of many individual "string" modes for this string, measured from plucks on the guitar as described earlier and used in Figure 6. The "floor" level of this scatter of points can be taken to indicate the intrinsic damping of the string. The open circles show a few values at higher frequencies, determined by bandwidth measurements from data like that plotted in Figure 2a. At such high frequencies the effects of body coupling are expected to be very small, as explained in the companion paper ([1, section 4.3]), so these values can be taken as representing string damping alone. The curve shows the best-fitted version of equation (8), with

values of the coefficients η_F, η_A and η_B as listed in Table I. It can be seen that the damping varies by an order of magnitude through this frequency range, and that the general pattern is matched reasonably well by the fitted curve. A few points around 4 kHz lie clearly below the fitted curve, but an explanation of this apparent anomaly will be given in section 4.3 below. Fits of similar quality have been obtained for the other five strings, and will be used in all simulations to be shown subsequently. Notice from Table I that all six strings required a value of η_B of the order of 2%, an intrinsically plausible value for a highly-aligned polymer.

4. Comparisons of measurements and synthesis

4.1. Comparison with the results from section 2

For this particular test guitar, it is now possible to synthesise pluck transients which will stand detailed comparison with the measured results described in section 2. The syntheses have been carried out using the frequency domain method described in the companion paper [1], with a sampling rate of 40 kHz to match the measurements, including body modes up to 11 kHz (480 modes) and string modes up to 18 kHz. As with the measured results earlier, it is hard to convey the overall picture with a small number of examples: each individual transient contains a lot of fine detail, and many notes and different plucking angles have been studied. As a first stage the two notes shown in Section 2 will be examined: the second fret on the fifth string and the open second string, plucked at 45°. In later subsections other notes will also be used, to illustrate aspects of the results not brought out by these first examples.

Figure 16 shows the first part of the time histories for these two notes, compared to the measured versions (upper traces) seen earlier in Figure 1. In both cases a general similarity can be seen, but the level of detailed agreement is not immediately impressive. The main pulses on the string, generated by the pluck and subsequently reflecting back and forth, can be seen in both experiment and theory. As discussed earlier, these pulses are expected to have "precursors" resulting from the dispersive effects of bending stiffness. These are more prominent in the syntheses than in the measurements, showing as bursts of high frequency before the main pulses. Such bursts are hardly visible at all in the measured waveform in Figure 16a, but in Figure 16b very clear similarities can be seen between measurement and synthesis. Between the pulses the response of the body modes can be seen, and again a certain level of agreement can be seen. The measurements and theory match well in the longer-scale patterns, suggesting that the low-frequency body behaviour might be captured accurately. The higher-frequency components are clearly different, but then the "statistical fitting" procedure used to obtain representative body behaviour at higher frequencies should not be expected to match the actual guitar in detail.

To see more clearly which aspects of the response are well modelled and which not, the results need to be analysed in other ways. Figure 17 shows the results of processing the first 10 ms of the data of Figure 16b using a sonogram with a very short time window. The sonogram amplitude is plotted with logarithmically spaced contours at 5 dB intervals. The highest contour is black, and lower ones are in progressively paler shades of gray. The most obvious features are curving ridges, which result from the "pulses" discussed above. These ridges follow closely the superimposed dashed lines, which indicate the theoretical times of arrival after the first two round trips on the string. The lines are curved because the high frequencies travel faster as a result of bending stiffness: the curved ridges are showing the detailed structure of the "precursors" mentioned above. The dashed lines were computed from the group velocity for the stiff string, using the values of tension, mass per unit length and bending stiffness as measured for this string and given in Table I.

The ridges are somewhat cleaner in the simulated case (Figure 17b), but are perfectly recognisable up to quite high frequencies in the measurement (Figure 17a). The

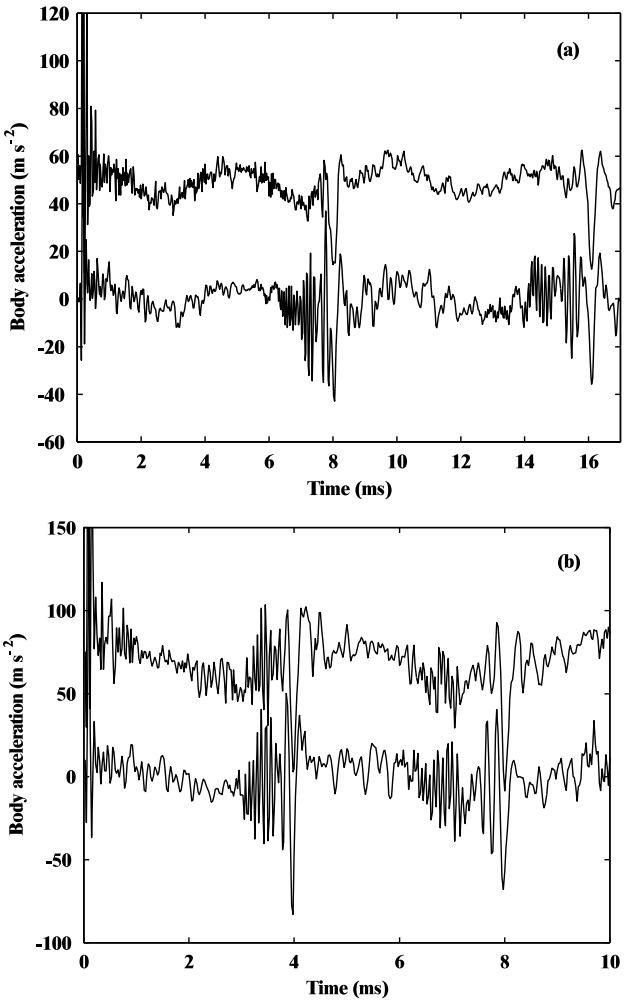

Figure 16. Measured (upper trace) and synthesised (lower trace) waveforms of guitar plucks from (a) B_2 on the second fret of the 5th string; (b) B_3 on the open 2nd string. The plucks were at a distance of 20 mm from the bridge and an angle of 45° to the soundboard. The measurements show the same data as in Figure 1.

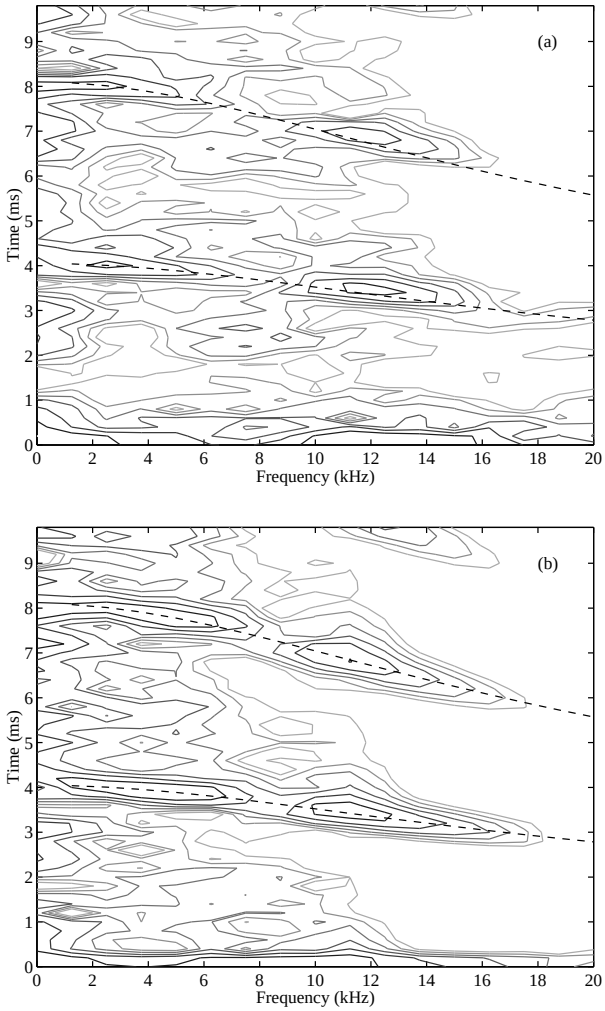

Figure 17. Sonograms of the plucks shown in Figure 16b (contour plots), for (a) the measured pluck and (b) the synthesised pluck. The highest contour is black, lower ones are spaced at 5 dB intervals and are in progressively paler shades of gray. Dashed lines show the expected arrival times of the main pulse excited by the pluck, after the first two round trips on the string. These lines are curved because of wave dispersion due to bending stiffness in the string.

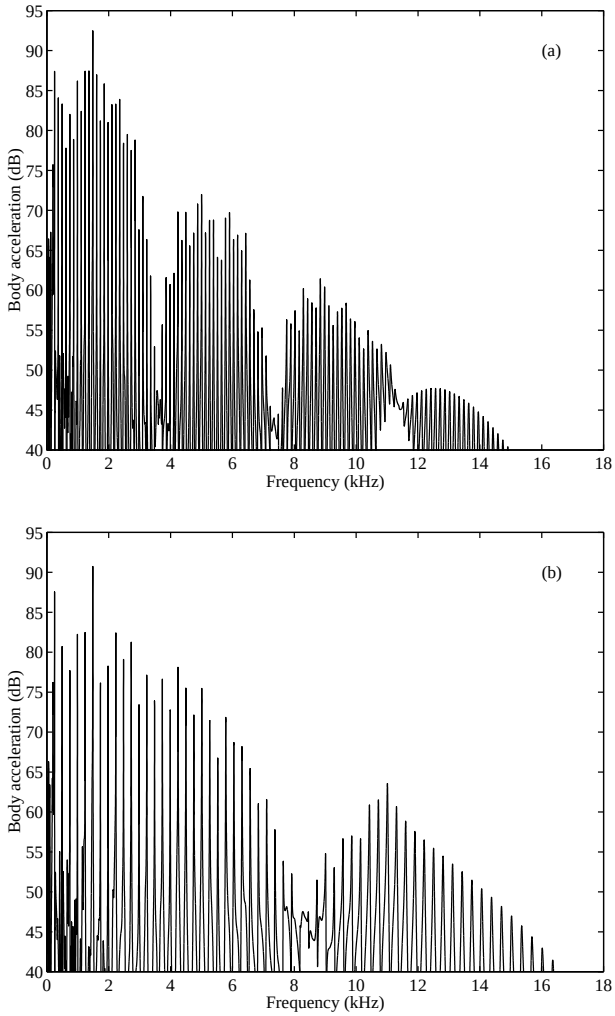

Figure 18. Frequency spectra of the synthesised plucks shown in Figure 16 from (a) B_2 on the second fret of the 5th string; (b) B_3 on the open 2nd string. The plucks were at a distance of 20 mm from the bridge and an angle of 45° to the soundboard. Scales are the same as for Figure 2.

modulation of the heights of the ridges, similar in both cases, is a result of the plucking point chosen for these tests. The dip in response around 8 kHz corresponds to the frequency at which the string modes first have a nodal point near the plucking position. The pluck position as a fraction of the string length was 20/650, and the inverse of this, approximately 32, gives the "harmonic number" at which a node will first be found at the plucking point. With a fundamental frequency at 247 Hz, this gives a frequency around 8 kHz, as observed.

Between the ridges the effects of body vibration are seen. At the very lowest frequencies, where the body response has been fitted in deterministic detail, the shapes of the high contours are recognisably similar between the two figures. At higher frequencies detailed agreement is not expected because of the "statistical fitting". Furthermore, the synthesis model only included body modes up to 11 kHz, so it is no surprise to see white space between the ridges of Figure 17b above that frequency. The fact that the contour structure of the right- hand end of the ridges is quite similar in the two plots gives a direct indication that the damping model for this string is working reasonably well at these high frequencies. On the whole, this figure tells a more encouraging story than Figure 16: aspects of the synthesis which should agree with the measurement are indeed doing so with reasonable accuracy.

In Figure 18, the frequency spectra of the two synthesised plucks are shown. These plots should be compared to Figure 2. Figure 19 shows some details from spectra at the three different plucking angles, in a format which is directly comparable to Figure 3. Figure 18a reveals that the synthesis has clear "string" peaks up to high frequencies, whereas the measurement in Figure 2a shows lower amplitudes above about 4 kHz and almost no visible peaks above 7 kHz. Even allowing for the noise floor in the mea-

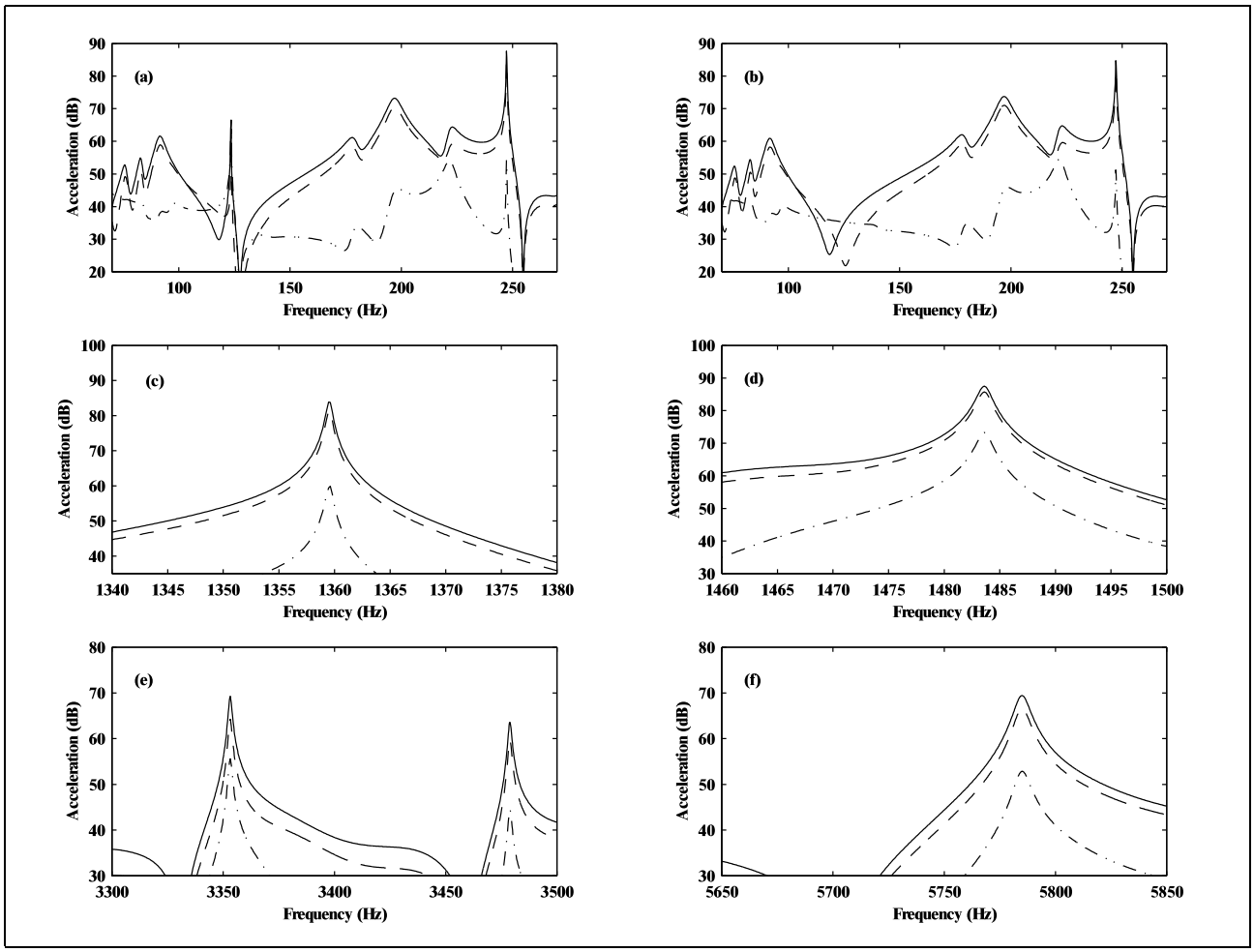

Figure 19. Details of frequency spectra of synthesised plucks: (a,c,e) B_2 on the second fret of the 5th string; (b,d,f) B_3 on the open 2nd string. In each case the solid line (usually the upper trace) shows a pluck normal to the soundboard, the dashed line (usually the middle trace) shows a pluck at 45°, and the dash-dot line (usually the bottom trace) shows a pluck parallel to the soundboard. The dashed lines show portions of the data from Figure 18. All scales are the same as for Figure 3.

surement, the frequency spectrum of the real pluck appears low-pass filtered compared to that of the synthesis. However, the comparison between Figures 2b and 18b shows, in general terms, a much closer match. The pattern of peak heights is reasonably similar up to the highest frequencies.

However, this broad view conceals many important details, some of which can be seen by comparing Figures 3 and 19. At low frequencies, both notes show rather good agreement with the measurements. The body mode amplitudes are about right, and the variation with angle of plucking is quite well reproduced, particularly for the plucks normal to the soundboard and at 45°. The plucks parallel to the soundboard produce significantly lower amplitudes, more so in the synthesis than in the measurement. It is possible that small deviations of the actual plucking angles from the intended ones can account for the disparity: the levels are extremely sensitive to angle near the parallel condition. Another conspicuous deviation between measurement and synthesis in this frequency range is that the "string" peak around 246 Hz is higher and narrower in both synthesised results, compared to the two measurements. The question of decay rates of low-frequency string modes will be considered in some detail in the next section, so this question is deferred for now.

Figures 19c,d show a more interesting deviation from the corresponding measurements. By this frequency, both measured notes showed a clear splitting of the "string" peaks by several Hz, whereas the syntheses show no visible splitting. The two polarisations of string motion are in fact split to form modes at different frequencies, but as was shown in Figure 8 of the companion paper [1], this predicted split is no bigger than 0.1 Hz, smaller than the bandwidth of the peaks and therefore not apparent in these plots. It may be noted in the measured results that the frequency corresponding to motion predominantly normal to the soundboard (solid lines) is higher in both cases than the frequency excited predominantly by plucking parallel to the soundboard (dash-dot lines). This pattern of peak splitting has been seen in very similar form for all notes analysed. More details and a possible explanation for this behaviour will be presented in section 4.3.

An even more striking disparity between measurement and synthesis in seen at higher frequencies, as shown in Figures 19e,f compared with Figures 3e,f. The synthesis

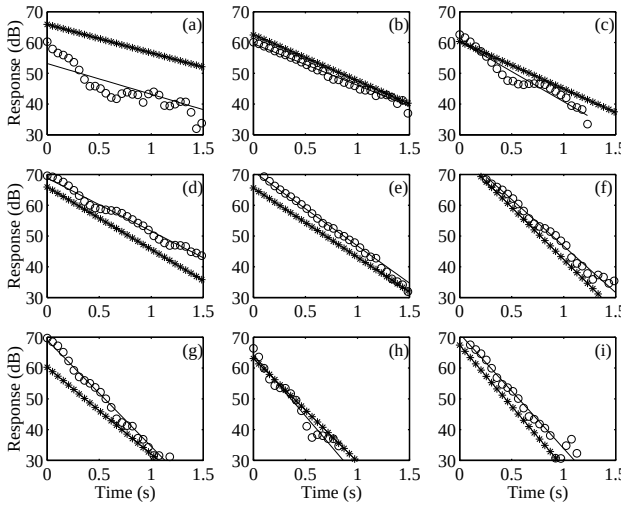

Figure 20. Decay profiles of the first nine "string" overtones for the open second string (B_3) plucked at 45° to the soundboard: measured (circles) and synthesised (stars). The measured data matches that shown in Figure 5. Best-fitted exponential decays are shown as straight lines.

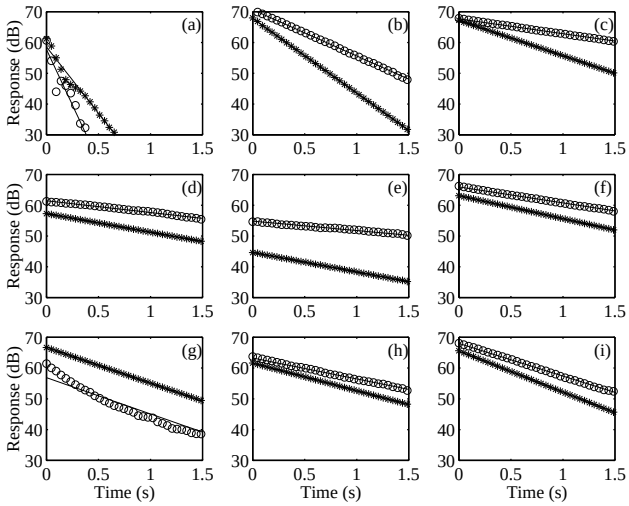

Figure 21. Decay profiles of the first nine "string" overtones for the second fret of the sixth string (F#) plucked normal to the soundboard: measured (circles) and synthesised (stars). The measured frequencies were 93.3 Hz, 184.3 Hz, 277.9 Hz, 370.1 Hz, 462.6 Hz, 555.4 Hz, 647.7 Hz, 740.6 Hz and 833.2 Hz respectively. Best-fitted exponential decays are shown as straight lines.

shows a very clean pattern, with "string" peaks in the expected positions, no visible splitting of peak frequencies, and a simple amplitude trend as the plucking angle is varied. The measurements show a bewilderingly complex pattern with many more peaks than seen in the syntheses. The theoretical model as used for these syntheses gives no clue about how such complex behaviour might arise, and it seems clear that a significant extension of the model will be needed to explain this behaviour. A likely explanation of this phenomenon, and an indication of how the model would need to be extended to take account of it, will be given in section 4.3.

It may be noted that, although the peak frequencies show the anomalous behaviour just described, the bandwidths of "string" peaks are approximately correct in all four comparisons of Figure 19c–f with the corresponding measurements. This confirms that the fitted damping model for the string is probably not too far wrong. This in turn suggests that the disparity of high-frequency roll-off between Figures 2a and 18a is not simply due to error in the damping model at higher frequencies. The evidence of peak bandwidths, and also the evidence of short-window sonograms like those shown in Figure 17, suggest that the general trends of damping are reasonably well matched by the fitted models. The origin of the disparity must lie elsewhere.

4.2. Decay rate comparisons

The next stage of comparison between synthesis and measurement involves the decay profiles of individual "string modes". Figure 20 shows results for the open second string plucked at 45°, with the measured results from Figure 5 superimposed. The fundamental of the note shows rather poor agreement, both in amplitude and initial decay rate, as was already guessed from the discussion of Figure 19b.

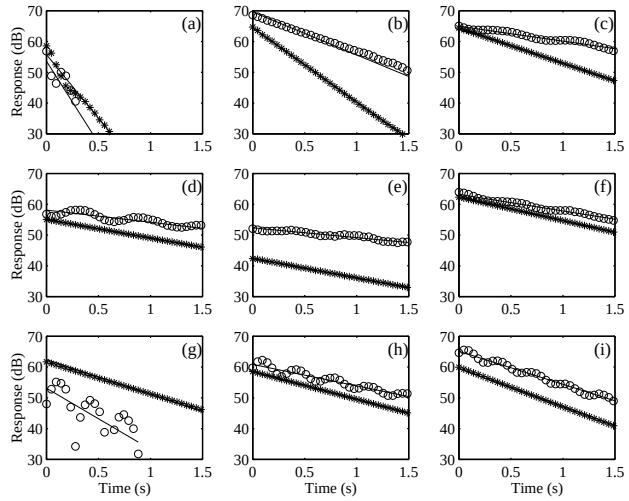

Figure 22. Decay profiles of the first nine "string" overtones for the second fret of the sixth string (F#) plucked at 45° to the soundboard: measured (circles) and synthesised (stars). Best-fitted exponential decays are shown as straight lines.

However, in most cases Figure 20 shows encouragingly good agreement . This general pattern is repeated for most notes studied: good agreement for many string frequencies, but occasional disparities, especially at lower frequencies. As was shown in the companion paper [1], body-coupling effects are expected to be most significant at low frequencies, so it is not surprising that the disparities are biggest there.

However, some notes show less good agreement, and it is worth illustrating one such case. Figure 21 shows results for the second fret of the sixth string (F#, 93 Hz) plucked normal to the soundboard, and Figure 22 shows the corresponding results for a 45° pluck. In both cases the

fundamental frequency shows quite good agreement with synthesis: at this frequency the string couples strongly to a body resonance, producing very rapid decay involving some beating behaviour. For most of the higher overtones shown here, Figure 21 shows decay profiles for both measurement and synthesis which are quite linear in the plot, in other words simple exponential decays. The initial levels are mostly in fairly good agreement, but several of the decay rates are clearly in error. Figure 22 shows a more striking effect: the synthesis results are very similar to those of Figure 21, but the measurements show, in several cases, very clear beating behaviour with beat frequencies of a few Hz. This beating is the time-domain manifestation of peak splitting like that seen in Figure 3c,d. It has already been noted that the synthesis model predicts splitting of much smaller magnitude, such that any beating would have a period of several seconds and therefore would hardly manifest itself before the note had decayed.

The reasons for the poor agreement in decay rates between measurement and synthesis in Figure 21, for example, are not entirely clear. One possibility concerns the fact that the synthesis method used here required the full 2×2 admittance matrix at the guitar bridge, and this was not measured on the same day as the pluck data was collected. Perhaps the guitar behaviour was slightly different on the two days, either because of changing humidity or because the effects of the support fixture were slightly different on the two occasions. However, the normal admittance Y_{11} *was* measured on the same occasion as the pluck data, without moving the guitar in the support fixture. This admittance can be used to synthesise pluck response in the normal direction, if the second string polarisation is ignored. The results of such a synthesis, not shown here, are very similar to those of Figure 21, and are not in any better agreement with measurement. It seems that physical changes to the guitar body between measurements are not the explanation for the incorrect decay rates.

Another possibility concerns small errors in string tuning, shifting the mode frequencies relative to nearby body modes. The strings were tuned using a commercial electronic tuner, but it is not clear what such a tuner responds to, when the string has significant inharmonicity due to bending stiffness. Figure 7 of the companion paper shows some relevant data for the variation of predicted decay rates with the precise frequency of the string, based on the same synthesis model as is being used here. It can be seen from that figure that the two overtones at 184 Hz and 278 Hz, with clearly erroneous decay rates, both lie close to body modes, so that sensitive variation might be expected. However, the fitted frequencies for these two overtones in the measurement differ from those of the synthesis by only about 1.5 cents, so although tuning error may account for part of the disparity of decay rates, it is not a strong enough effect to account for it fully.

Other possible explanations lie in inaccuracy of the fitted damping model for the string, and in non-linear effects to be discussed in section 4.3. At present there is not enough available data to test these possibilities quantitatively. To assess how serious these anomalies of decay rate are for the overall accuracy of the guitar synthesis, it is useful to turn from individual decay rates to summary plots for all "string modes" of a given string. Figure 23 shows results in the same form as Figure 6. Damping factors have been computed for each string, using frequency domain synthesis allowing for both string polarisations, and using the fitted frequency-dependent damping model for the string. The dashed line shows the measured results for comparison. The general features are well reproduced: the pattern of the "floor level", the positions of major peaks in loss factor at low frequencies, and the typical peak-to-valley variation across the whole frequency range shown. In Figure 23f for the lowest string of the guitar, notice that the anomalies at 184 Hz and 278 Hz discussed above correspond to regions where the two curves both have smooth shapes, but with levels differing by a factor 2 or so.

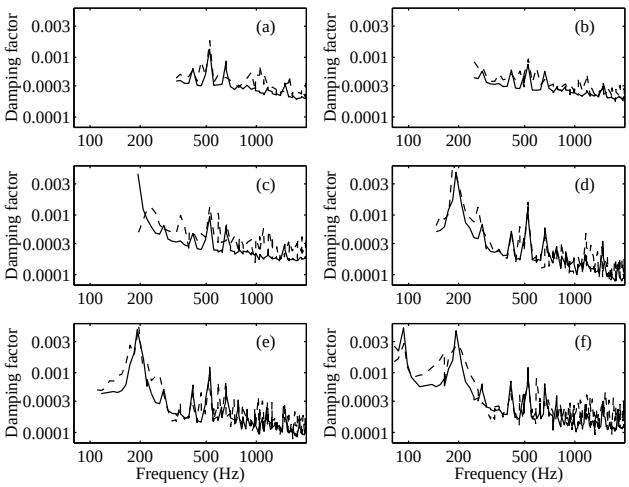

Figure 23. Damping factor as a function of frequency for "string modes" of all notes up to the 12th fret of the test guitar: measured (dashed lines) and synthesised (solid lines). Plots a–f correspond to strings 1–6 respectively.

Figure 24 shows comparative results using different synthesis methods, all applied to the sixth string of the guitar. Figure 24a repeats the data of Figure 23f, while Figure 24b shows the result of synthesis allowing only one polarisation of string motion, normal to the soundboard. Figure 24c shows results comparable to Figure 24b, but using the measured body admittance directly rather than the modally-fitted version (with its "statistical" element). This comparison is shown for the case of a single string polarisation only, because the measured admittance (Figure 7) for this case is more reliable than the measurement of the full admittance matrix. The fact that Figures 24a,b,c all show a very similar pattern of results suggests that, from the point of view of damping factors at least, (i) inclusion of the second polarisation makes rather little difference, and (ii) the modal fitting process, including the statistical element, was quite successful in producing a reasonable model. Notice that all three sets of results show deviations from the measured results with a similar pattern. Possibly the explanation for some of these deviations lies with

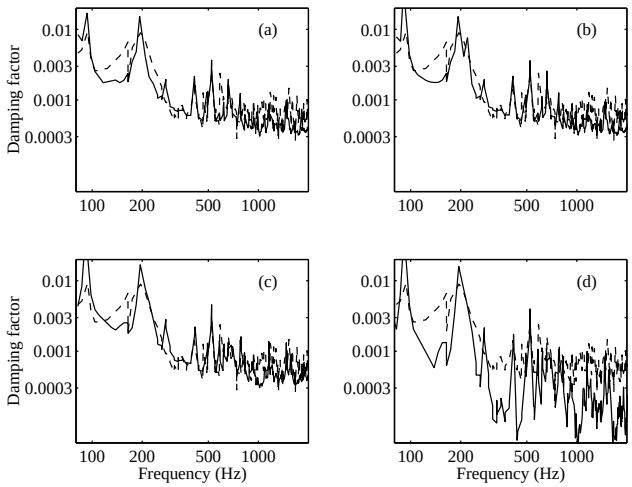

Figure 24. Damping factor as a function of frequency for "string modes" of all notes up to the 12th fret of the sixth string (E_1) of the test guitar: measured (dashed lines) and synthesised (solid lines) using different synthesis models. (a) Synthesis using both string polarisations, the fitted string damping model, and the modally-fitted admittance matrix shown in Figure 10 (as in Figure 23f); (b) synthesis allowing string motion in the plane normal to the soundboard only, with the fitted damping model and the modally-fitted admittance; (c) as (b) but using the measured admittance from Figure 7; (d) as (b) but using an undamped model for the string motion.

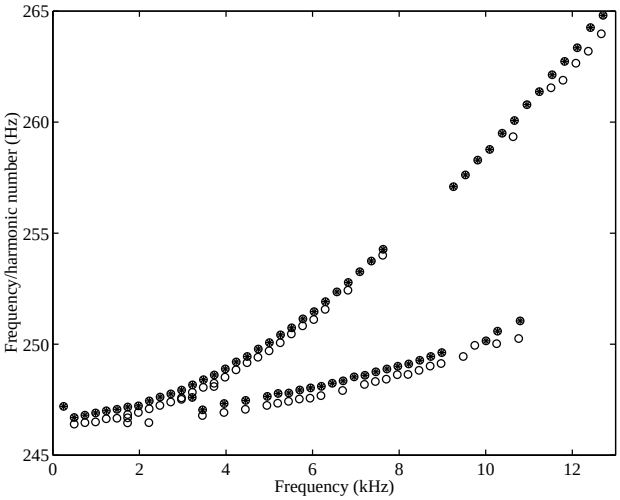

Figure 25. Frequency of "string modes" divided by "harmonic number" for plucks of the open second string (B_3), for all peaks which could be identified in the spectral data used for Figures 2b and 3b,d,f. Filled circles: peaks clearly visible in the spectrum of the pluck normal to the soundboard; open circles: peaks only clear in the spectra of plucks at 45° and parallel to the soundboard.

the measured decay rates rather than with the accuracy of the synthesis model: recall that these measurements were made under conditions resembling ordinary playing, via microphone signals in a normal medium-sized room, so it is possible that room acoustics effects have some influence. Finally, Figure 24d shows the result if the synthesis is carried out treating the string as undamped, as described in section 3.2 of the companion paper [1]. This time there is clearly a very big difference in the decay rates. The correct model for string damping is obviously a key ingredient of any accurate synthesis.

4.3. The pattern of "string peaks"

The most glaring anomaly not yet addressed concerns the comparison between Figure 3c–f and Figure 19c–f. The synthesis results show a simple and comprehensible pattern of almost-harmonic "string peaks", while the measurements show strong splitting into pairs of peaks, and later into more complex clusters apparently involving four or more peaks. To see what is happening in more detail it is useful to extend an analysis like that shown in Figure 13 to higher frequencies. The spectra of Figures 2b and 3b,d,f were searched carefully by hand to find all clear peak frequencies f_n. Each was associated with the apparently relevant "harmonic number" n, then f_n/n was plotted against f_n to produce the graph shown in Figure 25. Filled circles indicate peaks which were clear in the results for a pluck normal to the soundboard, while open circles show peaks only clear in the results for the plucks parallel to the soundboard and/or at 45°.

The results show a very striking pattern. The uppermost curve is the continuation of the one used earlier to fit the bending stiffness of the string: it can be seen clearly throughout this frequency range, except for the gap around 8–9 kHz where the plucking point was close to a nodal point on the string. This curve is "shadowed" by a parallel line of open circles, consistently a little lower in frequency. Another pair of curves appears lower in the plot, apparently emanating from the same frequencies at the left-hand side but curving upwards more slowly. This pair consists again of an upper curve of filled points, and a lower, parallel, curve of open circles. This clear, albeit puzzling, pattern shows that the random-looking pattern of peak splittings in the original spectra in fact contains considerable structure.

There are two aspects of these results to be considered, and tentative explanations will be advanced for both. First, consider the upper pair of parallel curves. What these appear to show is that the string vibrating in the plane parallel to the soundboard has a slightly greater effective length than the same string vibrating in the plane perpendicular to the soundboard. From the ratio of frequencies given by the separation of the curves, this difference of effective lengths is not very big: a matter of about 0.8 mm, in a string of length 650 mm.

This length difference is of the same order of magnitude as the diameter of the string, and an explanation may be found in the geometry of a string passing over a fret, as sketched in Figure 26. (Note that although this particular note was an open string, the test guitar has a "zeroth fret" so that the geometry is approximately the same for open and stopped strings.) For motion normal to the fret, there is no doubt that displacement must be zero (assuming the fret to be rigid) at the contact point marked "A".

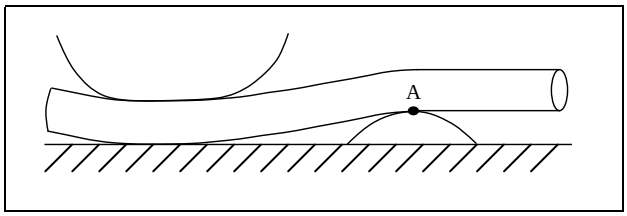

Figure 26. Sketch of the geometry when a string is held against a fret by a finger behind the fret in the usual way.

For motion of the string parallel to the fret, though, it is not so clear what the correct boundary condition should be. If there is no slip on the fret then the tangential displacement at point A on the string's surface will be zero, but the centre of the string could still move a little by rolling on the fret. It is easy to imagine an "end correction" of the order of the string diameter associated with this rolling motion. The exact amount would require detailed computation, and might well depend on the details of the player's fingering behind the fret: how close the finger end was to the fret, how hard it was pressed against the fingerboard, and the stiffness properties of the fingertip. A similar correction would apply at the bridge saddle, unless the saddle has a notch to inhibit rolling.

The main conclusion is that this effect, although small, produces a more significant influence on the interaction of the string polarisations than that coming from the body admittance matrix. The beating behaviour seen, for example, in Figure 22 is caused primarily by this end-correction effect. It seems quite likely that the beating has audible consequences, although whether this would be regarded as desirable or undesirable is hard to guess. It may be noted that the effect is similar to one reported by Erkut et al [20] for the strings of the kantele (a traditional Finnish plucked instrument). In that case, the manner of tying the strings at one termination produces different effective lengths for the two polarisations of motion, and the authors show that it is important to include the effect in a realistic synthesis model. The synthesis model used here could of course be modified to take account of the end-correction effect, but this possibility is not pursued here.

If this explanation is correct, and if the beating has audible consequences, then it is likely that different fingering techniques for a given note might produce perceptibly different sound qualities. It is usually assumed that, because the player's finger is behind the fret and therefore isolated from the vibrating section of string, details of fingering technique will not influence the sound. It now seems that this may not be true. This question may be one worthy of further study.

The second striking feature of Figure 25 is the appearance of a second pair of curves below the pair already discussed. The explanation of these becomes reasonably clear once it is realised that the second pair of curves is related to the first pair by scaling the frequency axis by precisely a factor of two. These additional points are frequency-doubled versions of points on the original curves, which must therefore be generated by a nonlinear mechanism. A link with nonlinearity is further confirmed by experiments (not reproduced here) in which the amplitude of string motion was varied: the anomalous peaks are less prominent when amplitudes are lower.

The obvious candidate for the source of nonlinearity, the simplest mechanism which can produce second-order terms, is excitation of longitudinal vibration of the string by the finite amplitude of the transverse vibration. These longitudinal waves can manifest themselves in the measured body acceleration, and in the radiated sound spectrum, via other terms in the bridge admittance matrix, not discussed so far. In reality this matrix is three-dimensional, and will have coupling terms between longitudinal and normal motion (Y_{13} in the notational convention used earlier). The action can be visualised qualitatively: tension variations in the string acting at the top of the bridge saddle cause some rotation of the bridge about its long axis, and this rotation will cause bending motion of the soundboard, and hence sound radiation.

The governing equations for the three-dimensional coupled finite-amplitude motion of a string are given by Morse and Ingard [21], see equation (14.3.7). The relevant approximation here is to regard the transverse motion as large, and to act as a driving term for the linearised equation for longitudinal motion. A further approximation is often made in the existing literature (e.g. [19, 22, 23]), to regard the driving force as coming from quasi-static tension variations calculated from the net increase in string length. However, it is not clear that this last approximation would be appropriate for a study of the phenomenon shown here, since the observed nonlinear peaks extend well up into the frequency range where longitudinal resonances of the strings can be expected. Indeed, there is a hint in some of the results of the present study that the prominence of the nonlinear peaks is modulated according to an underlying sequence of longitudinal string modes. However, detailed modelling of the phenomenon is not pursued here.

As with the beating arising from the end-correction effect, it seems likely that the multitude of frequency-doubled spectral peaks arising from this nonlinear mechanism might produce some audible consequences. Notice that it was only possible to identify these anomalous frequencies so clearly because of the effect of bending stiffness in the string. If the string overtones had been truly harmonic, the frequency-doubled components would have fallen on top of higher overtones of the original transverse series. The frequency-doubled series correspond to the overtone sequence of a string with the same fundamental frequency but a lower bending stiffness: the curvature of the quadratic function is governed by the value of B/T, from equation (6). Any attempt to explore the audibility of the effect should presumably take account of interaction with bending stiffness.

The nonlinear process under discussion here has a bearing on some anomalies of measured damping factors. First, if energy is being extracted from a given transverse string mode to drive longitudinal motion at twice the frequency,

this will inevitably increase the damping factor of the transverse mode. This may contribute to the difficulty of predicting decay rates accurately, discussed above. Secondly, the nonlinear effect explains an anomaly in the set of decay rates plotted in Figure 15. A few points around 4 kHz in that plot fell well below the fitted curve which was claimed to represent the string's intrinsic damping. However, examining the detailed results reveals that these points correspond to frequency-doubled components of the signal (i.e. to points on the lower pair of curves in Figure 25). If they are shifted back to their "true" positions around 2 kHz, they lie within the envelope of the other points and cease to present an anomaly. The decay rate of a frequency-doubled component is governed by the decay rate of the transverse string mode which is driving it.

5. Conclusions

A study has been presented in which the predictions of a synthesis model for the coupled string/body vibration of a plucked guitar note were compared with measurements. The model assumes that the vibration is linear, that the string vibration is governed by the usual wave equation augmented to include the effect of bending stiffness and a suitable frequency- dependent model for internal damping, and that the string is coupled at a single point to the body of the instrument. The body vibration is characterised by its admittance matrix at the coupling point, so that the interaction of the two polarisations of string motion via the body could be correctly modelled. All the parameters of the model were determined by careful measurements on the chosen test guitar.

Although the model just described seemed the "obvious" one, it proved to be only moderately successful at reproducing the detailed behaviour seen in measured plucks. A reasonably good match was found at low frequencies, except that individual decay rates of "string modes" were not all matched correctly. Even to get a match as good as has been demonstrated here, it is essential to use an accurate damping model for the string: the intrinsic damping of the classical guitar strings used here was found to vary by an order of magnitude in the audible frequency range, and if this variation is not included in the synthesis model, very poor predictions of decay rates are obtained.

At higher frequencies it was found that two phenomena not included in the synthesis model produced conspicuous disparities between measurement and synthesis. First, the polarisations of string motion normal and parallel to the soundboard gave modal frequencies which were split much wider apart than could be accounted for by body coupling. This effect is tentatively attributed to the detailed boundary conditions at the ends of the string, where slight rolling on the fret and/or bridge can result in different effective lengths for the two polarisations. The difference of effective lengths is not large: it is of the same order as the diameter of the string. However, this is enough to produce an effect which far outweighs the peak-splitting caused by coupling through the guitar body vibration.

The second conspicuous disparity concerns the pattern of peaks observed in frequency spectra: unexpected extra peaks were seen in the measured spectra, which are frequency-doubled relatives of the expected peaks due to transverse string resonances. The non-linear mechanism creating these additional peaks is presumed to involve excitation of longitudinal string motion by the transverse vibration. Such longitudinal motion can excite vibration of the guitar body through the linear vibration properties, so that these additional frequencies are seen in the structural vibration response to the pluck, and also in the radiated sound spectrum.

The shortcomings highlighted here of the "obvious" synthesis model are not exactly new ideas, but they do not seem to have been quantified with care in any previous study. Many workers in the field of guitar acoustics have observed peak-splitting, and the corresponding beating in the decay envelopes, but no-one seems to have observed that the magnitude of the splitting is not compatible with body coupling as the cause. Various authors have written about nonlinear vibration of strings, but only very limited information seems to have been published to show clear signs of it in radiated sound from normal playing on a classical guitar [24]. The frequency dependence of damping of musical strings has been in the literature for some time, but it is only rarely taken into account in the context of synthesis. The results presented here suggest that all these factors should be included in a synthesis model which is intended to produce accurate predictions.

A number of questions are raised by these results about the auditory significance of the phenomena seen in measurements. No attempt has been made here to assess whether the various effects described can be heard, but there is surely considerable scope for exploring these questions. How accurately must the individual decay rates of string overtones be reproduced in order that the sound is indistinguishable from the real pluck? Is peak-splitting due to string rolling, or additional spectral peaks due to nonlinearity, audible? If so, what is the perceived impact on tonal quality? Answers to these questions would have implications for makers and players of guitars, as well as for those concerned with high-quality synthesis for musical purposes, and the issues deserve further study.

Acknowledgement

The author thanks Bernard Richardson and Robin Langley for helpful discussions, and Martin Woodhouse for assistance and for providing the test guitar.

References

[1] J. Woodhouse: On the synthesis of guitar plucks. Acustica/acta acustica **90** (5).
[2] G. Weinreich: Coupled piano strings. J. Acoust. Soc. Amer. **62** (1977) 1474–1484.
[3] C. H. Hodges, J. Power, J. Woodhouse: The use of the sonogram in structural acoustics and an application to the vibrations of cylindrical shells. J. Sound and Vibration **101** (1985) 203–218.

[4] R. J. Hanson: Analysis of "live" and "dead" guitar strings. J. Catgut Acoust. Soc. **48** (1987) 10–16.
[5] A. Chaigne: Viscoelastic properties of nylon guitar strings. J. Catgut Acoust. Soc. Series II **1** (1991) 21–27.
[6] J. Woodhouse: On the playability of violins. Part I: reflection functions. Acustica **78** (1993) 125–136.
[7] D. J. Ewins: Modal testing: theory and practice. Research Studies Press, Letchworth, 1984.
[8] J. C. Schelleng: The violin as a circuit. J. Acoust. Soc. Amer. **35** (1963) 326–338.
[9] J. Woodhouse: On the playability of violins: Part 2, Minimum bow force and transients. Acustica **78** (1993) 137–153.
[10] E. V. Jansson: Experiments with violin string and bridge. Applied Acoustics **30** (1990) 133–146.
[11] E. V. Jansson, B. K. Niewczyk: On the acoustics of the violin: bridge hill or body hill. J. Catgut Acoust. Soc. Series II **3** (1999) 23–27.
[12] E. Skudrzyk: Simple and complex vibratory systems. Pennsylvania State University Press, Pennsylvania, 1968.
[13] C. Lambourg, A. Chaigne: Measurements and modeling of the admittance matrix at the bridge in guitars. Proc. Stockholm Musical Acoustics Conference 93, Royal Swedish Academy of Music Stockholm **79** (1993) 448–453.
[14] J. Woodhouse: Body vibration of the violin – what can a maker expect to control? J. Catgut Acoust. Soc. Series II **4** (2002) 43–49.
[15] M. L. Mehta: Random matrices. Academic Press, San Diego, 1991.
[16] G. Weinreich: Vibration and radiation of structures. – In: Mechanics of Musical Instruments. A. Hirshberg, J. Kergomard, G. Weinreich (eds.). Springer-Verlag, Vienna, 1995.
[17] Lord Rayleigh: Theory of sound, Vol. 1. Dover Publications, New York, 1945.
[18] H. Järveläinen, V. Välimäki, M. Karjalainen: Audibility of the timbral effects of inharmonicity in stringed instrument tones. Acoustics Research Letters Online **2** (2001) 79–84.
[19] C. Valette: The mechanics of vibrating strings. – In: Mechanics of Musical Instruments. A. Hirshberg, J. Kergomard, G. Weinreich (eds.). Springer-Verlag, Vienna, 1995.
[20] C. Erkut, M. Karjalainen, P. Huang, V. Välimäki: Acoustical analysis and model-based sound synthesis of the kantele. J. Acoust. Soc. Amer. **112** (2002) 1681–1691.
[21] P. M. Morse, K. U. Ingard: Theoretical acoustics. McGraw-Hill, New York, 1968.
[22] C. E. Gough: Nonlinear generation of missing modes on a vibrating string. J. Acoust. Soc. Amer. **76** (1984) 5–12.
[23] K. A. Legge, N. H. Fletcher: The nonlinear free vibration of a damped elastic string. J. Acoust. Soc. Amer. **75** (1984) 1770–1776.
[24] H. A. Conklin: Generation of partials due to nonlinear mixing in a stringed instrument. J. Acoust. Soc. Amer. **105** (1999) 536–545.